ENHANCED MICROWAVE ABSORPTION ON FORMULATED SiC/FELDSPAR COMPOSITE SUSCEPTOR

by

NURUL ZAFFIQA BINTI ZAMZURI

A report submitted in fulfillment of the requirements for the degree of Bachelor of Applied Science (Materials Technology) with Honours

FACULTY OF EARTH SCIENCE
UNIVERSITI MALAYSIA KELANTAN

2017

DECLARATION

I declare that this thesis entitled “Enhanced Microwave Absorption On Formulated SiC/Feldspar Composite Susceptor” is the result of my own research except as cited in the references. The thesis has not been accepted for any degree and is not concurrently submitted in candidature of any other degree.

Student

Name: Nurul Zaffiqa Binti Zamzuri

Date:

ACKNOWLEDGEMENT

First of all, I would like to take this great opportunity to express my sincere gratitude and thank you to my supervisor, Dr. Muhammad Azwadi Bin Sulaiman and my co-supervisor, Dr. Muhamad Najmi Bin Masri for their invaluable sharing of knowledge, comments, ideas and advices about this final year projects. There were very patient and concern about the problems that I have during the experimental progress and they also help to find the best solutions to overcome the problems to make sure that the project was succeed. Besides, they also love to share their previous experience during conduct the experiment to make sure that I do not repeat the same mistakes.

Secondly, I would like to thank to my parents, En. Zamzuri Bin Ali, Pn. Nora Binti Jamil and my siblings that always giving me moral supports and always understand my situation during my final year progress. They also always giving me advices to focusing and did efficient work since Final year project I.

Then, I also want to give a thousand thank to all my friends in UMK Jeli Campus especially for Siti Zuraina Binti Nawawi, Nurul Ainon Binti Bakar and Nor Khairiyah Azra Binti Kamiran, Wan Marinah Izzati Binti Wan Ismail, Brandon Lim Cheun Jie and Ezzaruddin Bin Eezahan that also help me during experiment progress and giving me continuous supports. They were very kind to teach me how to use a few machines and software to make me work faster without making any mistakes. Besides, we also like to share knowledge to improve our working skills.

Finally, I would like to separate my sincerest gratitude to all my course lecturers, faculty of earth science and laboratory assistants whom were always willing to help, advices and share their knowledge to me to finish up this writing and experiment successfully. Then, I dedicated this thanks to all people that helped me directly and indirectly during my writing and experiment progress.

Enhanced Microwave Absorption On Formulated SiC/Feldspar Composite Susceptor

ABSTRACT

In this research, SiC/Feldspar composite used to exam to see the potential of the material to absorb heat and save the energy used so it was tested to a few different compositions (x = 10,20, 30, 40 and 50wt%) of feldspar and the best composition was being tested with the microwave absorption and porosity also density measurement. From the replication process, it can show that whether the density and porosity measurement is influenced with the microwave absorption factor or vice versa. Finally, each of the process progress, the XRD technique will be used to identify the phase identification. Besides, optical microscope also be used to identify the microstructure of the product. As a result, it shown that the SiC-20wt% feldspar composite was good composition compared to others after the microwave absorption technique and it shown that the bulk density of SiC-30wt% feldspar composite was the lighter sample recorded was 0.048 g/cm^3. Besides, for apparent porosity, SiC-20wt% feldspar composite was the lower amount recorded which was 21.8%. Based on the result in this research, it can be said that the SiC-20wt% feldspar composite susceptor by using slip casted method was the best product.

Mempertingkatkan Penyerapan Gelombang Mikro Pada Rumusan Susceptor SicC/Feldspar Komposit

ABSTRAK

Dalam kajian ini, SiC/Feldspar komposit diuji untuk melihat potensi bahan yang menyerap haba dan menjimatkan tenaga yang digunakan maka jadi ia telah diuji untuk beberapa komposisi yang berbeza (x = 10,20, 30, 40 dan 50wt%) daripada feldspar dan komposisi yang terbaik sekali lagi diuji dengan penyerapan gelombang mikro dan keliangan pengukuran ketumpatan. Dari proses pereplikaan, ia menunjukkan sama ada pengukuran ketumpatan dan keliangan dipengaruhi dengan faktor penyerapan gelombang mikro atau sebaliknya. Akhir sekali, setiap keputusan, teknik XRD akan digunakan untuk mengenal pasti fasa yang wujud. Selain itu, mikroskop optik juga digunakan untuk mengenal pasti mikrostruktur produk. Hasilnya, ia menunjukkan bahawa SiC-20wt% feldspar komposit adalah komposisi yang terbaik berbanding dengan orang lain selepas teknik penyerapan gelombang mikro dan ia menunjukkan bahawa ketumpatan pukal SiC-30wt% feldspar komposit adalah sampel yang lebih ringan yang direkodkan ialah 0.048 g/cm^3. Selain itu, untuk keliangan ketara, SiC-20wt% feldspar komposit adalah jumlah yang lebih rendah dicatatkan iaitu 21.8%. Berdasarkan keputusan dalam kajian ini, ia boleh dibuktikan bahawa SiC-20wt% feldspar komposit susceptor dengan menggunakan kaedah tuangan slip adalah produk yang terbaik.

TABLE OF CONTENTS

TITLE	PAGE
DECLARATION	**ii**
ACKNOWLEDGEMENT	**iii**
ABSTRACT	**iv**
ABSTRAK	**v**
TABLE OF CONTENTS	**vi**
LIST OF TABLES	**ix**
LIST OF FIGURES	**x**
LIST OF ABBREVIATIONS	**xii**
LIST OF SYMBOLS	**xiii**
CHAPTER 1	**1**
INTRODUCTION	**1**
1.1 Background of Study	1
1.2 Problem Statement	4
1.3 Objective	5
1.4 Expected Outcome	5
CHAPTER 2	**6**
LITERATURE REVIEW	**6**
2.1 Introduction	6
2.2 Ceramic Composite Susceptor	9
2.3 Properties of Ceramic and Composite Ceramic	11
CHAPTER 3	**15**
MATERIALS AND METHOD	**15**
3.1 Introduction	15
3.2 Raw Materials Characterization	15

3.3 Processing Method 17
3.4 Material Characterizations 21
3.4.1 Phase Analysis 21
3.4.2 Density and Porosity Measurement 21
3.4.3 Microwave Absorption 22
3.4.4 Microstructure 23
3.4.5 Dielectric properties 23
CHAPTER 4 **25**
RESULTS AND DISCUSSION **25**
4.1 Raw Material Characterizations 25
4.1.3 Microstructure of Sponge 28
4.2 Phase Identification After Mixing Process 29
4.3 Composite Characterization 31
4.3.1 Microstructure 31
4.3.2 Phase Analysis 32
4.3.3 Microwave Absorption 35
4.3.4 Density and Porous 36
4.3.5 Dielectric Properties 38
4.4 Susceptor Produced from Slip Casting and Sponge Replication 40
CHAPTER 5 **42**
CONCLUSIONS AND RECOMMENDATIONS **42**
5.1 Conclusions 42
5.2 Recommendations for A Future Research 43
REFERENCES **44**
APPENDICES B **50**
RAW DATA **50**
APPENDIXES C **54**

SAMPLE PRODUCTS AND TESTING **54**

LIST OF TABLES

No.	TITLE	Page
3.1	Composition of SiC/Feldspar composite	17

LIST OF FIGURES

No.	TITLE	Page
2.1	Conventional heating and microwave heating patterns	9
2.2	A) CNT B) Spherical powder C) Diamond D) Graphene E) Graphite. Where the red spot is hot and blue spot is cool	10
2.3	Typical tensile properties of a porous-matrix CFCC in both ±45˚ and 0˚.90˚ orientation	12
2.4	Density variation against percentage addition of Al-6% Si alloy	13
2.5	XRD pattern of microwave sintered a) pure Al b) Al-5wt%$Ni_{50}Ti_{50}$ c) Al-wt%$Ni_{50}Ti_{50}$ d) Al-15wt%$Ni_{50}Ti_{50}$ e) Al-20wt%$Ni_{50}Ti_{50}$	14
3.1	Silicon carbide powder	16
3.2	Feldspar powder	16
3.3	The research flow chart of processing of SiC/Feldspar composite susceptor	20
4.1	XRD pattern for raw materials	27
4.2	Microstructure of sponge	28
4.3	Average of sponge pore size	29
4.4	XRD pattern of SiC/Feldspar composite after mixing process	30
4.5	20x magnification by optical microscope a) SiC-10wt% feldspar b) SiC-20wt% feldspar c) SiC-30wt% feldspar d) SiC-40wt% feldspar e) SiC-50wt% feldspar	32
4.6	XRD pattern of SiC/Feldspar composite after sintering process at 1050˚C	34
4.7	Graph of temperature vs time for sintering process in 12 minutes	36

4.8	Bulk density of SiC/Feldspar composite	37
4.9	Apparent porosity of SiC/Feldspar composite	38
4.10	Dielectric constant of SiC/Feldspar composite	39
4.11	Dielectric loss SiC/Feldspar composite	40
4.12	Comparison between slip casted and sponge replication susceptor for microwave absorption testing	41

LIST OF ABBREVIATIONS

Al	Aluminium
Al_2O_3	Alumina
CFCCs	Continuous fiber-reinforced ceramic composites
CMC	Ceramic matrix composite
CNT	Carbon nanotubes
CVD	Chemical vapor deposition
EDX	Energy dispersive X-ray analysis
MMC	Metal matrix composite
$Na_2(SiO_2)$	Sodium silicate
PET	Polyethylene terephthalate
PMC	Polymer matrix composite
POP	Plaster of Paris
PVT	Physical vapor transport
SEM	Scanning electron microscope
SiC	Silicon carbide
TNT	Trinitrotoluene
UTM	Universal testing machine
XRD	X-ray diffraction

LIST OF SYMBOLS

%	Percentage
˚C	Degree Celsius
MHz	Mega Hertz
GHz	Giga Hertz
wt%	Weight percent
GPa	Gigapascal
≈	Almost equal to
˚	Degree
MPa	Megapascal
g/cm^3	Gram per cubic centimetre
a.u.	Arbitrary unit
Cm	Centimetre
mL	Millilitre
m_o	Weight of composite in the air
θ	Theta
μm	Micrometre

CHAPTER 1

INTRODUCTION

1.1 Background of Study

Composite material is a combination macroscopically (Tiwari, 2015b) at least two or more chemically insoluble and distinct phase to produce useful products (Hu, 2006). Composite consist of one or more reinforcement which is discontinuous phase provides stiffness, strength (Campbell, 2010), transfer the strength to matrix and load carrying that embedded with matrix which is continuous phase which protects the fibres from environment and abrasion also to maintain the distribution of fibres to improve the features by combine the different materials to produce new product with new excellent properties (Hu, 2006) and high performance. The example of matrix that applied in industries are ceramic, polymer and metal also the reinforcement that always be used are polyester resins, epoxy, vinyl ester resin, phenolic resin and polyimides (Cornsweet, 1970).

The main purpose of composite material is to produce new better properties of the products to make sure that it is suitable to be applied in real life. There are many properties that can be improved such as the strength and stiffness of the material and it can be stronger than metal with very light in weight (Mazumdar, 1998). Other than that, thermal conductivity, electrical conductivity and toughness (Tiwari, 2015a) of the composite materials is much better than certain metals. The combination of two phases help to modify the properties that suitable to be applied in industry.

Composite have a few classifications which are ceramic matrix composite (CMC), polymer matrix composite (PMC) and metal matrix composite (MMC). CMC is a heterogeneous material which the second phase (reinforcement) is embedded with a ceramic matrix that act as a primary phase (Low, 2014). Then, for PMC, it is an organic polymer that act as a matrix which have good adhesion properties and fiber act as a reinforcement where it very good in strength and modulus (Wang *et al.*, 2011) and for MMC it is where the matrix and reinforcement are exhibits many desirable properties especially mechanical properties to become attractive for structural of engineering applications (Venkatesh & Harish, 2015). All of this types of composite have their own speciality to be used in industries to improve the performance and productivity of the products by improve the properties of the material.

Nowadays, composite is one of the very famous material to be applied in many type of industries because it can create great properties and characteristics in the products that we wanted to use. In aerospace industry, the reinforcement that usually used is polymer (Hu, 2006) because it lightweight, multi-role or functionality, passenger safety, and aerodynamic performance (Vinet & Zhedanov, 2010). The example of application part that applied were rocket engines, radar, satellite structures, solar reflectors and antenna structures (Hu, 2006). Besides, it also be used in automotive industry such as engines, bodies, connecting rod and bearing materials that almost 100% of the material came from composite (Hu, 2006). Others, composite also widely used in aircraft industry such as jet engines, turbine shafts, flight control surfaces, landing gear doors and engine bay doors (Hu, 2006) (Cornsweet, 1970).

Silicon carbide (SiC) a compound of carbon and silicon that also known as carborundum (Moissan, 1907) which very important non-oxide ceramic in industrial applications (Gerhardt, 2011). SiC is very essential in industrial applications because

of the exclusive properties such as high erosion resistance, oxidation resistance, high melting point, chemical and thermal stability, high hardness and strength (National & Recherche, 2008) high temperature electronic devices and high power (Gerhardt, 2011). The exclusive properties can withstand rough or unwanted condition such as thermal and stress exposed. SiC susceptor need to be sintered at high sintering temperature which about 2000˚C (Sulaiman *et al.*, 2014).

The most common SiC formed are include whiskers, fibers, powders, coating and single crystals. There are several methods that can be used to produce SiC depending on the product form demand and its application (Plains & Plains, 2012). There are several techniques that can be used to produce single crystals of SiC such as physical vapour transport (PVT), chemical vapour deposition (CVD), sol-gel processing technique for synthesizing SiC, liquid phase sintering SiC technique and mechanical alloying process for SiC synthesis (Gerhardt, 2011).

Feldspar is a common raw material used in the glass making derived from German word is *Feldspat,* that combine from Feld word means 'field' and Spat word means 'rock that does not contain ore', the changes word from *Spat* to *spar* was influenced from the English word *'spar'* which means mineral (Marx, 1992). This mineral consist of tectosilicates that have a few major elements which are potassium-feldspar (K-spar) endmember $KAlSi_3O_8$, Albite endmember $NaAlSi_3O_8$ and Anorthite endmember $CaAl_2Si_2O_8$ (Marx, 1992). In the industry application, feldspar are used in pottery manufacture for white ware and vitrified sanitary (Deposits & Maine, 1906).

1.2 Problem Statement

SiC is a raw material that very suitable to be used by produce susceptor because of the mechanical properties that give a better result and good performance. Unluckily, to produce SiC susceptor, it need to sinter high temperature at up to 2000˚C so that it need very high cost of production and at the same time the energy produced is ineffective. To avoid very high cost of production, SiC powder will be mixed together with secondary phase as a binder. Besides, by applying a binder it can help to improve the properties of the products to become much better than previous.

In this research, feldspar is chosen to be the secondary phase that have a high potential to make a better innovation in susceptor application. By applying SiC with feldspar the sintering temperature were decreased to 1300˚C so that the cost of production can be decreased (Galusek *et al.*, 2014). At the same time, the properties of products by combining two main materials will create exclusive properties that can give a perfect performance.

The commercial SiC susceptor nowadays is a solid material that have a lower surface area. The composite susceptor of SiC/Feldspar will produce high porous structure and increase the total surface area by using sponge replication. As the result, it can increase the energy conversion which give an effective energy during the combustion process.

In addition, for future product, the physical and mechanical properties of SiC susceptor need to be improved to make sure that the product presentation was in better condition. At the same time, it can give many benefits to the user during applying the product.

1.3 Objective

The objective of this research are:

i. To synthesize SiC/Feldspar composite at different composition and forming method.

ii. To determine the characteristics of SiC/Feldspar composite using optical microscope, XRD, microwave absorption and dielectric test.

iii. To evaluate the efficiency of microwave absorption on slip casted susceptor and sponge replication.

1.4 Expected Outcome

At the end of this research, the different of ratio composition between SiC/Feldspar composite of each sample and the method that will be used can be identify which one is optimize with the electromagnetic absorption. Besides, by enhanced electromagnetic absorption of SiC/Feldspar composite susceptor, it can help to improve the productivity of products by reduce the production cost by lowering the sintering temperature during the process in industries.

CHAPTER 2

LITERATURE REVIEW

2.1 Introduction

Ceramic matrix composite is commonly composite for good insulators, low density, thermal stability and high stiffness products. The combination of ionic and covalent bonding between non-metal and metal elements are applied for turbine coatings (Naga, 2014), metal cutting (Zhao, 2014) and dental ceramics (Yin & Stoll, 2014).

Metal matrix composite is designed by the metal alloy as matrix and volume fraction, material type and form ceramic reinforcement such as cemented carbides and other cermets (Mazumdar, 1998). The products that produced from this composite can help to improve mechanical properties such as stiffness, fatigue resistance, creep, hardness, abrasion and wear resistance. The composite also can be operated of combine with the higher operating temperature than an unreinforced metal (Adams, 1987). This type of composite has high potential to be applied in military such as high-temperature fighter aircraft engines and naval weapons systems (Jones, 2001).

Polymer matrix composite is matrix material are from polymer based resin with some form of fibres embedded in matrix as reinforcement (Tejaswi, 2012). In applications, it widely used in commercial aircraft such as helicopters (Chawla, 2012). Clearly, PMC are major used in vehicles because excellent corrosion resistance and weight saving (Tejaswi, 2012).

In this chapter, the previous research about the making of susceptor will be reviewed. These reviews can be compared to identify which of the method or combination elements that can give a perfect presentation in real life to apply in industry. From this research, better susceptor can be created by improving the properties of the materials to help the heating process undergo with efficient way and safe to be used. Overall, the previous review can help to make a better product with many advantages such as low production cost and effective method processing.

Before microwave are widely used in the domestic microwave oven, electromagnetic spectrum form the microwave have been used in radar (Mecânica *et al.*, 2015), detection of submarines and enemy aircraft during Second World War in radar technology (Wong & Gupta, 2015). Besides, at the end of World War II, the researchers have been identified the potential of electromagnetic spectrum to be used in alternative application such as treatment food, wood and commercial processing, drying of tiles and textiles (Wong & Gupta, 2015) that very effective to be used. According to the (Cesnek *et al.*, 2003), the susceptor products have been used with microwave since late 1970s for applied in households. At the beginning, there are many types of susceptors have been tested but only those consisting of polyethylene terephthalate (PET) film lightly metallized with aluminium laminated element are suitable to be applied in the industries. The research keeps continuing to know the ability of the susceptor that influence with the thickness metallization and the morphology also electric of susceptors during the heating process by another researcher to reach the maximize potential of the microwave heating technique to be apply in the industries.

Based on the Figure 2.1, Bhattacharya & Basak, 2016 reported, the microwaves heating is much better than conventional heating because it have an ability to heat the

materials by based on molecule interactions with the electromagnetic field which the uniformity and speed of the heating process is more efficient. In other words, the conventional heating products will transfer the heat from the hotter surrounding environment and through mass and heat transfer mechanisms proceeds from the surface of hotter exterior surface to the interior of cooler product (Perry & Lentz, 2009). Besides, the microwave heating can replaced the cavity air with the outside air for several times per minute just to avoid excessive condensation on the walls of cavity (Perry & Lentz, 2009) and energy transfer instead heat transfer where the heating process was started from the material interior body (Mecânica *et al.*, 2015). From that, it clearly shown that microwaves heating has many advantages such as it can heated the materials rapidly, selectively and uniformly, also can reduced hazards to environment and human and enhanced life quality and reduced the cost of processing and quality of product production (Clark *et al.*, 2000). Additionally, it also can be enhanced finer microstructures and densification rates for microwave sintering and can minimize the thermal stresses because of the volumetric heating and unique nature of homogeneous upon heating process (Demirskyi & Vasylkiv, 2016).The frequencies of electromagnetic waves are between 300 MHz and 300 GHz that known as a microwave which the heat can be trapped inside the materials likes reaction of combustion synthesis. Nowadays, since the microwave application was widelt used for a cooking oven,the frequency used was degined at 2450 MHz for culinary industry (Mecânica *et al.*, 2015).

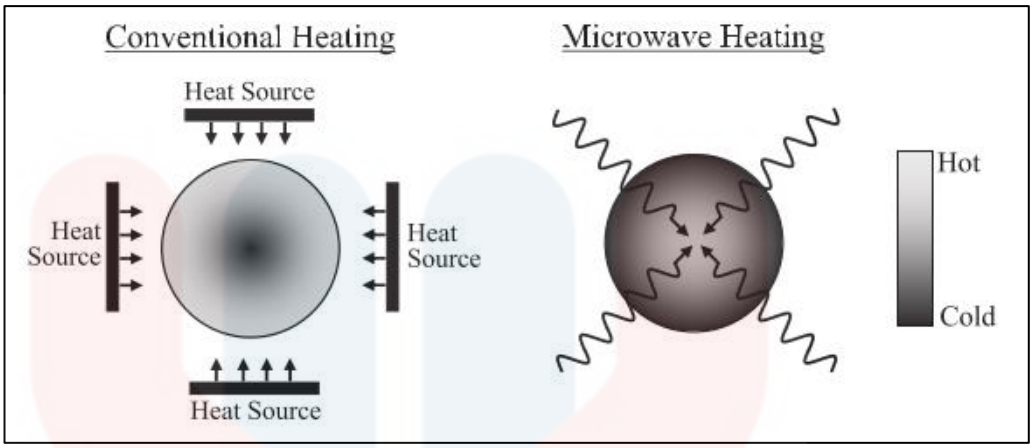

Figure 2.1: Conventional heating and microwave heating patterns (Bhattacharya & Basak, 2016)

2.2 Ceramic Composite Susceptor

According to the previous research by Sulaiman *et al.*, 2014, SiC and Al_2O_3 were combined to form a new composite to be applied in microwave heating because of the properties of SiC which have high melting point for casting and high susceptibility properties. Based on the report, the concentration of SiC and Al_2O_3 to investigate which of the ratio can indicating highest heating rate. The highest heating rate was crucible of 40 wt% SiC. The conclusion of this research, when the temperature was increased, the dielectric loss also increased and its accelerated the microwave energy conversion to heat.

A microwave-assisted has been developed to reach high quality multiferroic composites of $x\ Co_{0.65}Zn_{0.35}Fe_2O_4$ (CZFO)–(1-x) $PbZr_{0.52}Ti_{0.48}O_3$ (PZT) by (Mandal & Nath, 2014). The multiferroic composite materials containing ferromagnetic and piezoelectric phases with magnitude magnetoelectric that have been used in attractive applications such as microwave electronics, transducers, magnetoelectric sensors and resonators. Overall in this research, content of ferroelectric phases was the main influences in dielectric properties and based on the M-H loop measurements, when the

composites contain high ferrite amount so that the coercive field and the saturation magnetization also high.

Research by Vargas *et al.*, 2016 tested whether the carbon additives were influenced to Trinitrotoluene (TNT) to absorb microwave energy and heating throughout the composite. The carbon additives that used in this research were diamond nanoparticles, graphene nano-flakes, graphite micron-flakes, spherical powder and carbon nanotubes. In this research, all of the composite samples were attenuated microwave energy and exhibited volumetric heating except diamond nano-particles, so that it did not have a thermal heating behaviour in this experiment. Interestingly, carbon nanotubes (CNT) and graphene additives give hot spots at 60s of microwave exposure and it was produce TNT melting during microwave exposure shown as Figure 2.2. In conclusion, it shown that the shape of the susceptor play an important role to make the heating process work efficiently with monomolecular explosive, TNT.

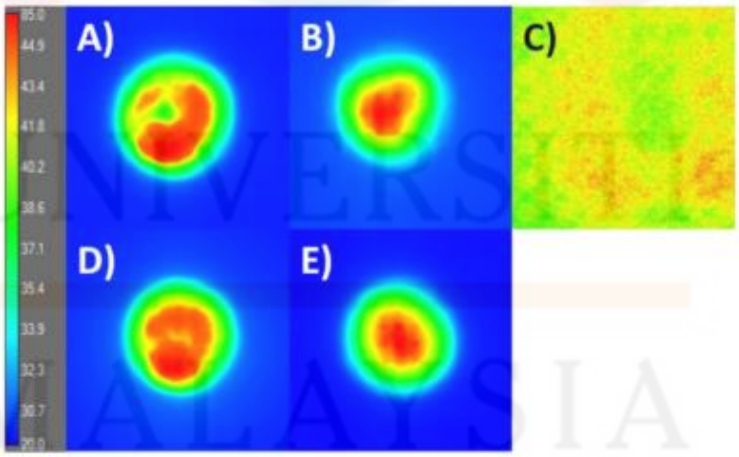

Figure 2.2: A) CNT B) Spherical powder C) Diamond D) Graphene E) Graphite. Where the red spot is hot and blue spot is cool (Vargas *et al.*, 2016)

Based on Clark *et al.*, 2000 research, the sintering process was tested on the alumina plates that used as an armor in military applications. The microwave hybrid

heating was used to rise the sample more than 1000˚C where the sample start to absorb the microwave energy itself because alumina has low-loss values of the dielectric loss factor. Based on the Archimedes method that used for measure density and strength factors, the soak temperature of sample was up to 300˚C lower than conventional method. These results shown that when the sample size was increased so the density of cross-sectional uniformity and sample density also increased, it because when the phenomenon inside of the sample was allowed to achieve high density before the density of surface layers, the internal porosity will minimize since the porous were trapped inside of the sample.

2.3 Properties of Ceramic and Composite Ceramic

After the processing method, the properties of the sample need to characterize to identify each of the properties that influence the result of the sample. One of the essential factor that need to be examined was density and porosity measurement. Based on the previous research by Sharmiwati, Mizan, 2014, it was studied about various solid loadings and polymeric sponge in the ceramic sponge properties. At this journal review, it was based on the density, porosity and mechanical properties whether it is effects of solid loadings quality and polymeric sponge or vice versa. According to the result, the density of ceramic sponge increases when the pore size of ceramic sponge increases. This hypothesis occurred because of the slurry was easily enter the form structure cause of the low viscosity of the ceramic, while the impregnation will affect when solid loading was high. Besides, when the pore size was increased, the linear shrinkage increased. It because of the particles of polymeric sponge was removed after the sintering process that made the holes became smaller and shrink the foam.

The research about the ceramic composite was become further when Baldacim *et al.,* 2001 was continuing the new founding about the porous matrix of the continuous fiber-reinforced ceramic composites (CFCCs). In this research, Baldacim *et al.,* 2001 was using a typical tensile properties to know the Young's modulus information based on the stress against strain graph. By referring Figure 2.3, the Young's modulus reading was E ≈ 60-11- GPa and the ultimate strength was $\sigma_u \approx$ 140-220 MPA. It can be concluded that the ±45˚ orientation, the composite have a lower ultimate strength of tensile and elastic modulus than the values corresponding in the orientation of 0˚/90˚ while it has a greater capacity for an inelastic straining. So that, the trend of the graph for 0˚/90˚ orientation was directly proportional of the stress against the strain while the trend of the graph for ±45˚ orientation was increased slowly at the beginning and remain constant at the 0.11% of strain.

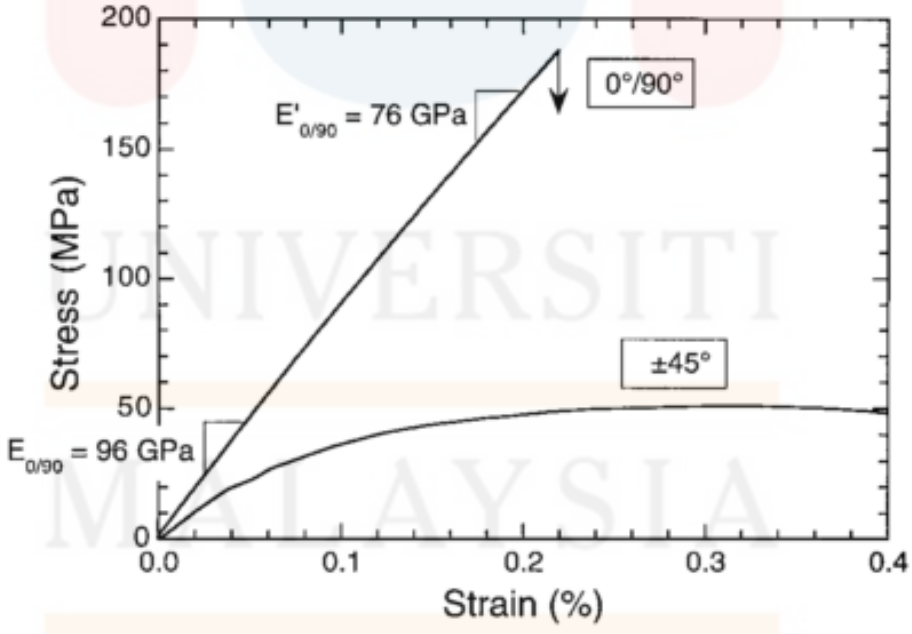

Figure 2.3: Typical tensile properties of a porous-matrix CFCC in both ±45˚ and 0˚.90˚ orientation (Baldacim *et al.,* 2001)

The density testing that already tested by Aigbodion *et al.,* 2011 with addition of Al-Si alloy. From these results on the Figure 2.4, it shown that the presence of alloy has little effect on the ceramic matrix composite density so it is because the trend of the graph decreased slowly until the density reach 2.75 g/cm^3. In this research, the density of unreinforced for tin tailings particles was 2.95 g/cm^3.

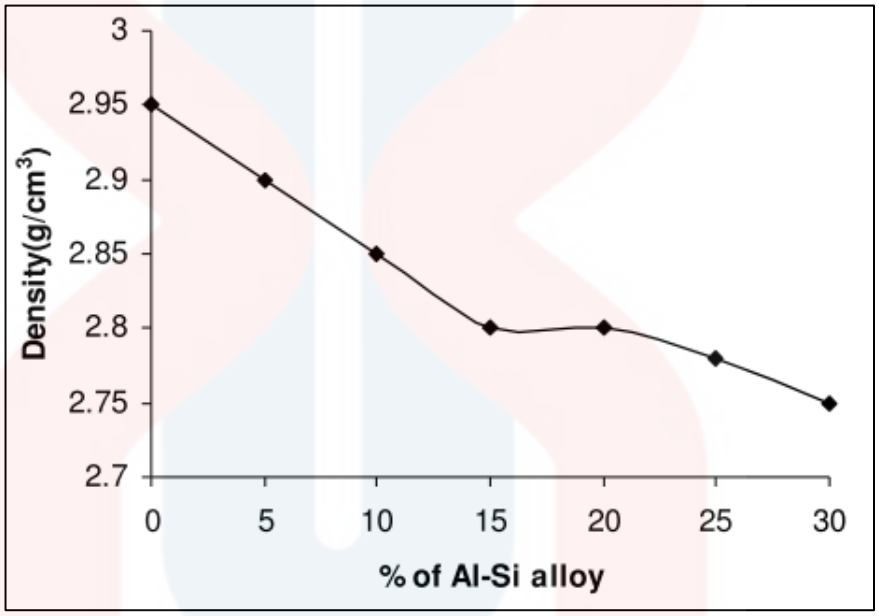

Figure 2.4: Density variation against percentage addition of Al-6% Si alloy (Aigbodion *et al.*, 2011)

According to the previous research by Reddy *et al.,* 2016, which based on the Al-$Ni_{50}Ti_{50}$ composite which was categorized as MMC. This composite was chosen because of the light weight, better mechanical and tribological properties. Besides, Al-$Ni_{50}Ti_{50}$ was one of the composite that can be controlled the reinforcement size and volume fraction. Based on the Figure 2.5, the sample of pure Al and Al composites was tested by using XRD analysis. This analysis can be helped to observe all the corresponding peaks to the pure Al and Al composites phases due to the shorter sintering process time because of the heating rate was accelerated. According to Reddy *et al.*, 2016, FCC was the phase identification that indicates the Al peaks and any secondary phase that absence.

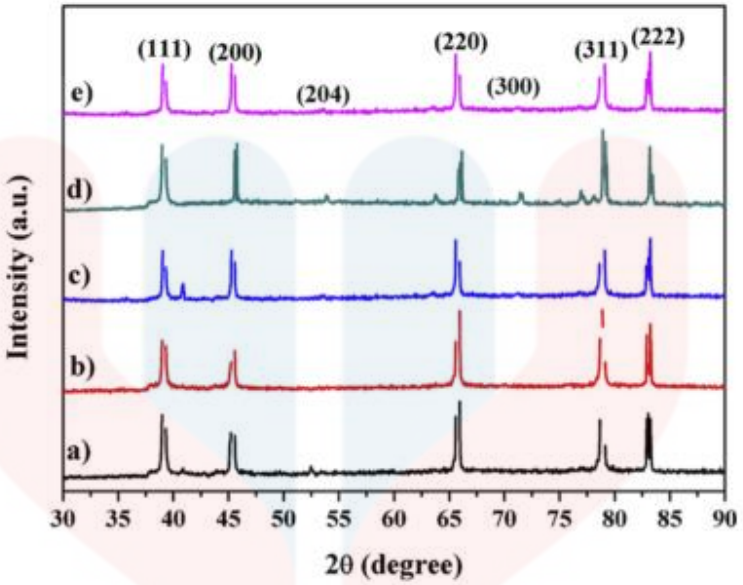

Figure 2.5: XRD pattern of microwave sintered a) pure Al b) Al-5wt%$Ni_{50}Ti_{50}$ c) Al-wt%$Ni_{50}Ti_{50}$ d) Al-15wt%$Ni_{50}Ti_{50}$ e) Al-20wt%$Ni_{50}Ti_{50}$ (Reddy *et al.*, 2016)

CHAPTER 3

MATERIALS AND METHOD

3.1 Introduction

In this chapter, its explain the materials and methods that will be used to conduct the experiment. The main raw materials in this research are SiC and feldspar will be manipulated in term of weight to produce different composition of SiC/Feldspar composite. To create sponge replication process, the solid-state reaction will be conducted for making the polycrystalline solids at 1000˚C to 1500˚C from a solid starting materials mixture. Then, there are a few testing will be followed such as microstructure, phase analysis, density and porosity measurement, and electromagnetic absorption to know the characteristic of composite product. Finally, the microwave absorption process will conduct once again to differentiate the heat absorption between slip casting sample and sponge replication sample method.

3.2 Raw Materials Characterization

SiC powder as shown as Figure 4.1 used to act as a matrix with 400 mesh particle size where it can be as a degradative resistance that cause structure failure such as chemical attack, water absorption, impact damage and high temperature creep (Chawla, 2012).

Figure 3.1: Silicon carbide powder

Feldspar as shown as Figure 3.2 was a material that act as a reinforcement where it used to improve the fracture toughness to provide the stiffness and strength that were lack in the matrix phase (Chawla, 2012). The chemical composition for this raw material as $KAlSi_30_8$ where it known as a potassium feldspar.

Figure 3.2: Feldspar powder

To analyse the raw materials, optical microscope and X-Ray Diffraction (XRD) technique will be chosen to identify the characteristics of feldspar and SiC. All these initial techniques will help to compare with the final product of composite in order to identify the changes of the characteristics.

The analysis study by Bruker, D2 Phaser Powder Diffractometer was used to characterize of feldspar and SiC powder. 10˚ to 90˚ scanning angle was used to examine the phase present in the materials and the X-ray diffraction pattern was identified by using DIFFRAC.EVA software to compare the elements in the initial phases for both raw materials.

The optical microscope is a chosen technique to explain about the morphology of the sponge which the shape of the porous. Besides, this technique helps to determine the dimension of porous that having at a sponge to know the average porous contain.

3.3 Processing Method

Raw materials of SiC and feldspar need to be analysed by using XRD technique before convert into composite material. In Table 3.2, the main raw materials were weighted for 5 compositions accurately and mixed homogenously using magnetic stirrer for an hour by followed (x= 10, 20, 30, 40 and 50) wt% ratio of feldspar. Then, during the mixing process, 80 mL of distilled water was used as an optimum medium to help the raw materials mixed easily on the hot plate. In addition, $Na_2(SiO_2)$ was added about 1 mL that function as a binder to help for both of the raw material bind well. Each of the composition was once again needed to analyze by using XRD technique to identify the percentage contain of elements in the materials after mixing process.

Table 3.1: Composition of SiC/Feldspar composite

Feldspar powder (wt %)	Silicon carbide powder (wt%)
10	90
20	80
30	70
40	60
50	50

Each of the composition sample was shaped by using POP mould to produce susceptor and the pellet shape mould was proceeded by hydraulic hand press for other materials study. After that, the sample needed to through firing process in the furnace. At 1050˚C with 12 hours running process, the sample need to fire to get the rigid shape. Then, the samples needed to be characterized using a few techniques to determine new properties after heat treatment process. There were a few techniques such as XRD, density and porosity microstructure, optical microscope and microwave absorption. After all the techniques were used, the best composition of the sample will be used to be proceed with another step.

The best composition of the sample was proceeded with the replication process where the sponge was used to make porous structure on the sample. After that, the sample was through firing process by using furnace with 1050˚C and 12 hours heating again to have a rigid shape. Then, the sample were characterized again using microwave absorption to identify the amount of heat absorption to be compared with the slip casted technique.

This processing method was referred by Sulaiman *et al.*, 2014. The process by making composite product was solid state reaction and follows the research flow chat in Figure 3.1

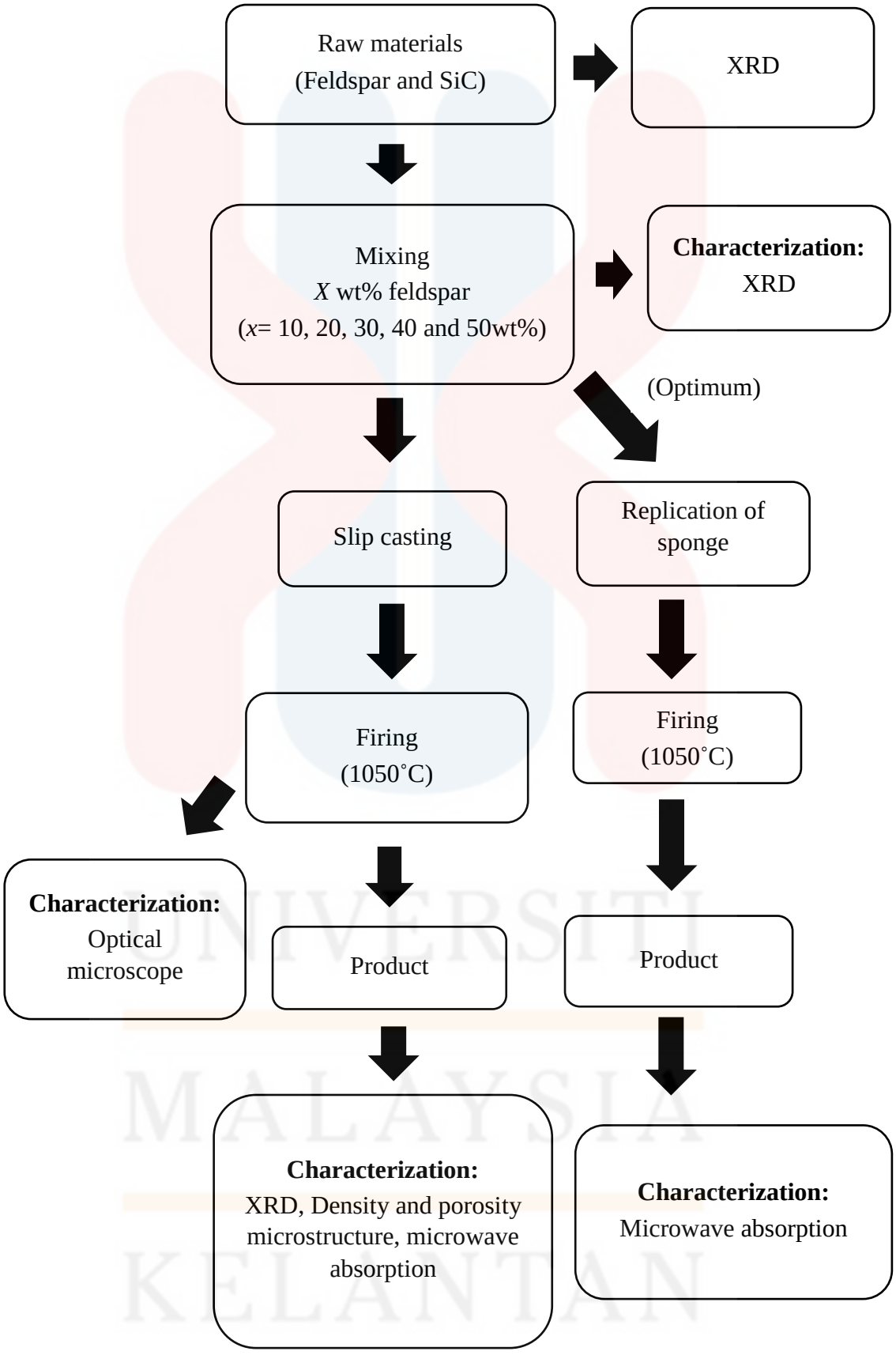

Figure 3.3: The research flow chart of processing of SiC/Feldspar composite susceptor

3.4 Material Characterizations

In this session, there are a few techniques that was used to identify the material characteristics of sample such as XRD, density and porosity measurement and microwave absorption.

3.4.1 Phase Analysis

The raw materials and composite composition of SiC/Feldspar was analysed using XRD with the powder sample. This technique helps to identify the percentage of crystallinity, the (h, k, l) values, lattice parameter, size and also determine the element contain of the materials by using DIFFRAC.EVA software. Besides, this technique was used to confirm the phase formation and material properties based on the XRD pattern and database finding.

3.4.2 Density and Porosity Measurement

Then, to measure the density and porosity, the samples were prepared in pellet shape using hydraulic hand press. Each of the SiC/Feldspar composite need weighted and the measurement should be recorded. Desiccator in the vacuum was used if any of the air bubbles are trapped and the function was to remove it to avoid the sample react with water from humidity. Then, the final weight of the SiC/Feldspar composite need to weight once again. The Archimedes's principle was applied to measure the bulk density and apparent porosity of the SiC/Feldspar composite (Sulaiman *et al.*, 2014). The bulk density was calculated by referring Equation 3.1.

$$\text{Bulk density}, \rho = \frac{D\ X\ \rho(\text{water})}{W - s} \qquad (3.1)$$

where

$\rho(\text{water})$ = Density of water (g/cm^3) = 1.00 g/cm^3

D = Dry weight, (g)

W = Saturated weight, (g)

Besides, the apparent porosity will be calculated by using Equation 3.2, where it was to compare the porosity percentage against different dopant concentration.

$$\text{Apparent porosity} = \frac{W-D}{W-S} \text{ x100 \%} \qquad (3.2)$$

where,

D = Dry weight, (g)

W = Saturated weight, (g)

S = suspended weight, (g)

3.4.3 Microwave Absorption

Each of the sample was tested using microwave oven that connected with the thermocouple and the temperature controller which was displayed the temperature reading when testing was running. In this testing, the sample will be heated for 12 minutes to record the increasing temperature for each of 30 seconds. From this testing, it can showed that the best of microwave absorption properties were attributed to high electric resistivity and excellent electromagnetic impendence (Guo *et al.*, 2011).

3.4.4 Microstructure

In this technique, it was used optical microscope to see the microstructure after firing process and also image of sponge by using Jenoptik software. From the image, it can show the microstructure structure of the grain boundaries of the sample with 20x magnifications clearly and the same time it also can measure the size of porous sponge by using the microscope in sponge replication process.

3.4.5 Dielectric properties

The purpose to identify of dielectric properties was to understand the interaction between microwave and materials (Fagury-Neto & Kiminami, 2001). Using microwave sintering, it can show the internal interactions of the microwave with the ions, atoms and molecules from the material when the heat was generated.

Based on the Equation 3.3, 3.4 and 3.5 it shown that the related between the capacitance and dielectric constant. Based on the equation stated, it can be assumed that when the capacitance increased, the amount of dielectric constant also increases. By relating the dielectric constant and dielectric loss, it can predict that when the dielectric constant increased, the dielectric loss also increase.

$$C = \varepsilon_{\circ} \frac{A}{l} \qquad (3.3)$$

$$C = \varepsilon_{\mathrm{r}} . \varepsilon_{\circ} \frac{A}{l} \qquad (3.4)$$

$$\varepsilon_{\mathrm{r}} = \frac{Cl}{\varepsilon_{\circ} . A} \qquad (3.5)$$

where,

C = Capacitance, (F)

A = Surface area, (m)

l = Thickness of the pellet, (m)

ε_o = Universal constant, (8.85^-12 F/m)

ε_r = Dielectric constant

CHAPTER 4

RESULTS AND DISCUSSION

4.1 Raw Material Characterizations

In this research, the raw materials that used were Si and feldspar that will be mixed to form new composite material. Both of the raw materials were examined by using XRD technique to identify the characteristics and element contain in the material.

Based from the Figure 4.1, the XRD spectra of SiC was measured in arrange of 2θ = 10˚ to 90˚ which shown that SiC with COD 9010158 (moissanite). The crystallinity contain in SiC was 85.2% and the amorphous contain was 14.8%. Besides, the crystalline structure of this raw material was hexagonal. Besides, the value of lattice parameters for a and c were 3.081 and 15.12480 respectively. From Figure 4.1, it shown a few clear peaks that have a sharp and weak diffraction peak. The highest peak that contain in the graph was at 2θ = 35.7˚ with (102) while the lowest peak that contain in the graph was at 2θ = 73.3˚ with (203). Besides, the first peak that shown in the graph is at 2θ = 34.1˚ where the hkl reading is (101) while the next peak after the highest peak is at 2θ = 38.1˚ with (103) and at 2θ = 41.4˚ with (104). Next, at the 2θ = 60˚, the intensity that recorded was (210) while the 2θ = 65.6˚ with hkl reading was (109) and at 2θ = 71.7˚ with (216).

According to Figure 4.1, the XRD spectra of feldspar was measured in arrange of 2θ from 15˚ to 55˚ which shown that Feldspar with COD 9004191 (microcline) was act as a primary phase and COD 9013308 (anorthoclase) was as weak secondary phase.

The crystalline contain in feldspar was 78.6% and the amorphous contain was 21.4%. Figure 4.1 proved that the primary phase contains more peaks than secondary phase. The lattice parameter of a and c for primary phase was 8.57140 and 12.96460 respectively. Besides, the lattice parameter for secondary phase of a was 8.27800 and for secondary phase of c was 12.94900. According to the Figure 4.4, the highest peak that recorded in this graph was at 2θ = 27.4˚ at (002) and the lowest peak was at 2θ = 41.9˚ with (060) and 2θ = 51.1˚ at (204). The second highest peak was at 2θ = 27.4˚ with (220). Others, at 2θ = 21.7˚ the hkl value was (201), at the 2θ = 25.5˚ with (212) and 2θ = 30.7˚ with hkl value was (131). Lastly, at 2θ = 27.8˚ with (002) where it is only the secondary phase peak that recorded. In conclusion, SiC that act as a matrix material was only contain primary phase while feldspar that act as a reinforcement was contain primary and secondary phases.

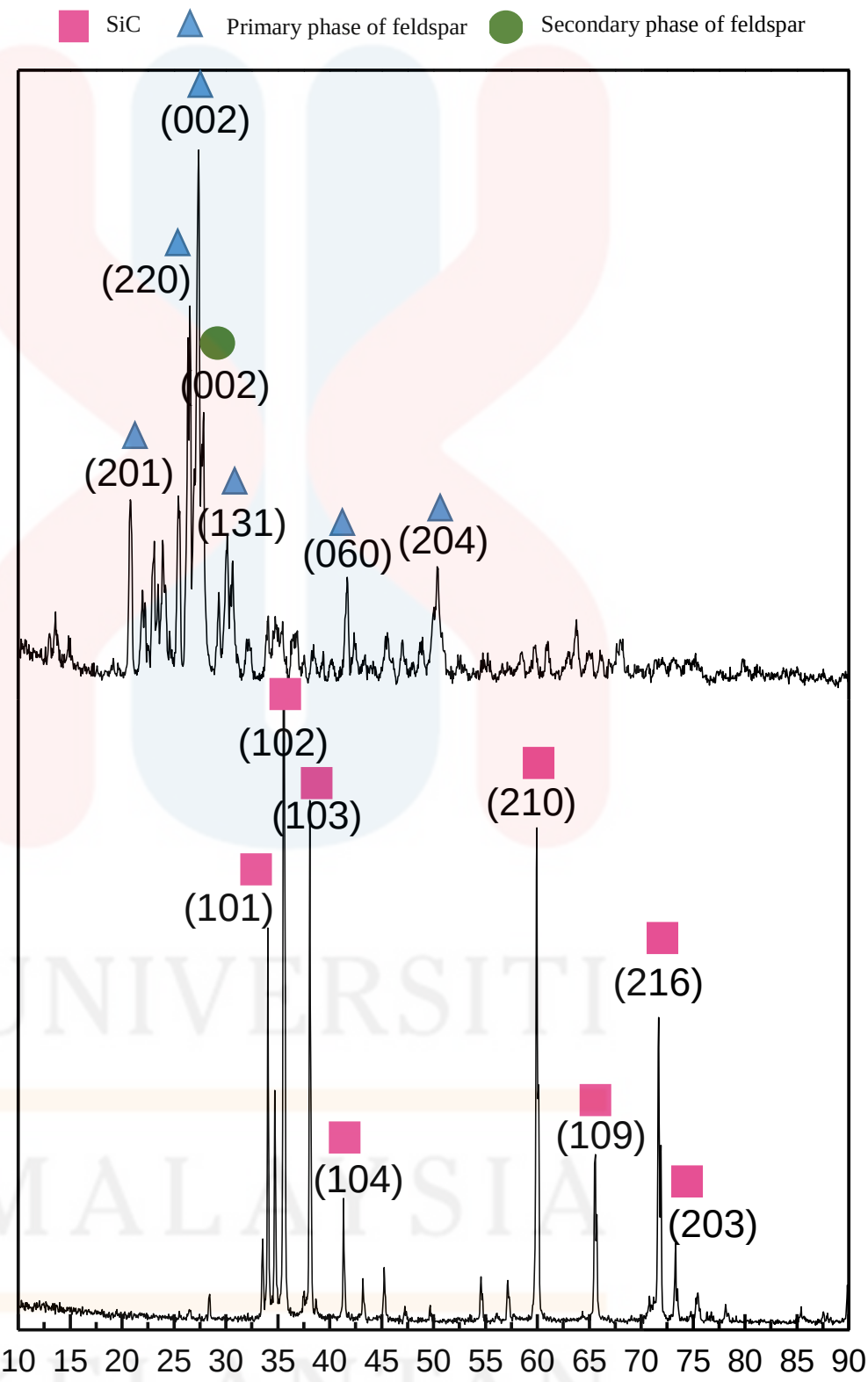

Figure 4.1: XRD pattern of raw materials

4.1.3 Microstructure of Sponge

Based on the Figure 4.2, it shown that 30 number of pores sponge that can be calculated using optical microscope. Purpose of this technique was to identify the average and the exact shape of pore sponge. The scale that used for this measurement was 2000 μm with 5x/0.1 magnification for each types of sponge.

Refering the Figure 4.2, it shown that the shape of the sponge was non-uniform. Some of the shape was circle, rectangle and pentagon shape.

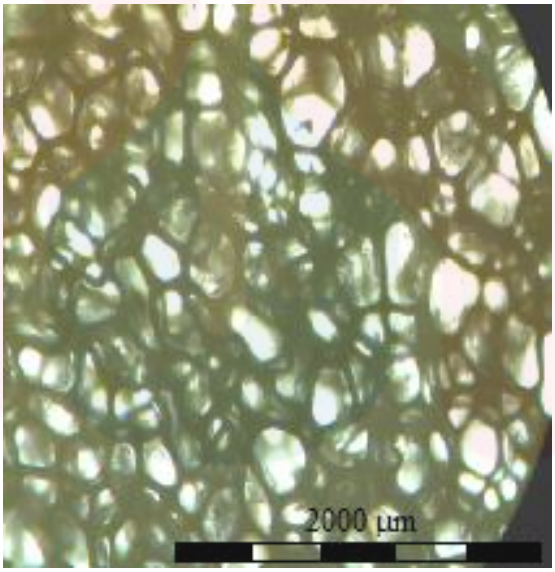

Figure 4.2: Microstructure of sponge

Figure 4.3 shows the average sponge pore size that have been measured between the pores. This measurement was very essential because it can influence the microwave absorption during the testing where the early hypothesis it can be said that the smallest pores can gives a better result because of the higher surface area.

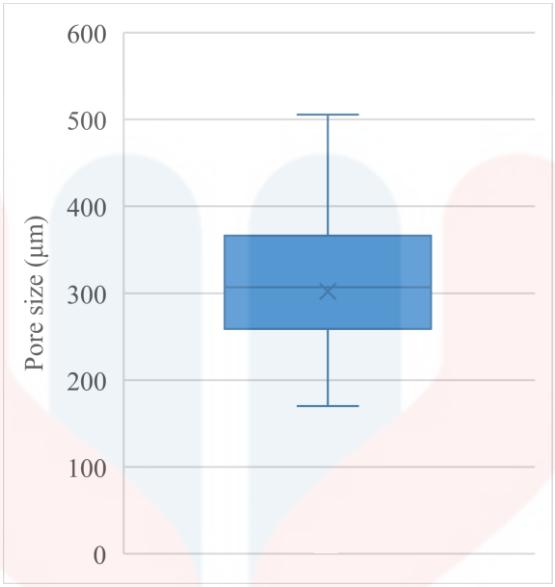

Figure 4.3: Average of sponge pore size

4.2 Phase Identification After Mixing Process

XRD technique was conducted after the mixing process by using magnetic stirrer. The purpose to do this technique again was to make sure that there was no any chemical reaction on the raw materials after the mixture process.

Figure 4.4 shows the XRD spectrum of the SiC/Feldspar composite after the mixing process. The XRD technique was measured in arrange of $2\theta = 15^{\circ}$ to 90° which shown that SiC with COD 9010158 (moissanite) and feldspar with COD 9004191 (microcline) and COD 9013308 (anorthoclase) phases combined together according to the composition provided. The SiC was having more peaks than feldspar so that this result was synchronized with the parameter of composition.

Comparing the XRD pattern from raw materials and after mixing process, it shown that most of the highest peak was from SiC and the rest of the peak was from the feldspar. In conclusion, most of the hkl of this process was majorly same with the previous raw materials.

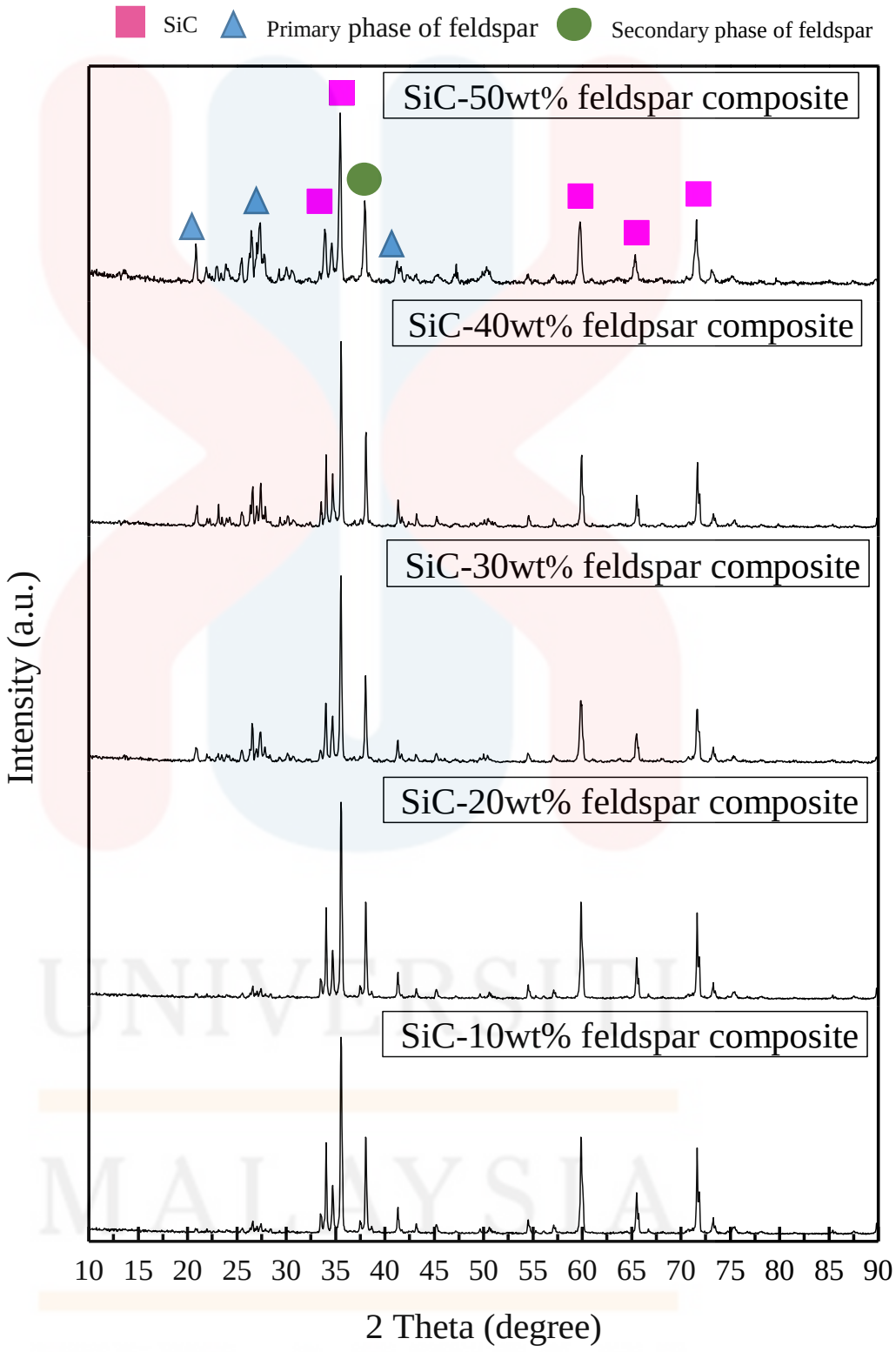

Figure 4.4: XRD pattern of SiC/Feldspar composite after mixing process

4.3 Composite Characterization

After the SiC/Feldspar composite was produced there were a few testing techniques were conducted to identify and determine the characterization of the final product such as optical microscope, XRD, microwave absorption and density and porosity measurement.

4.3.1 Microstructure

Microstructure using was 20x magnification will be used to see clearly is shown in Figure 4.5.

Based on the Figure 4.5 a), it was shown that the SiC-10wt% feldspar composite has shape of grain boundaries which not sinter into each other and there still have air gap between the powder particle. According to Figure 4.5 b) which is SiC-20wt% feldspar composite, the grain does not have regular shape. In other words, some of the grain have a big shape and some was vice versa. The inconstant shape of grain it shows that the grain in this sample was many compared with another sample. Based on the Figure 4.5 c), it shown that the SiC-30wr% feldspar composite has shape of grain and air gap between the powder particle was do not same with each other. Based on the Figure 4.5 d), it shows that the SiC-40wt% feldspar composite has shape of grain and air gap between the powder particle was do not same with each other. Lastly, Figure 4.5 e) show that the 20x magnification of SiC-50wt% feldspar composite where the shape of grain was not having the regular shape with each other.

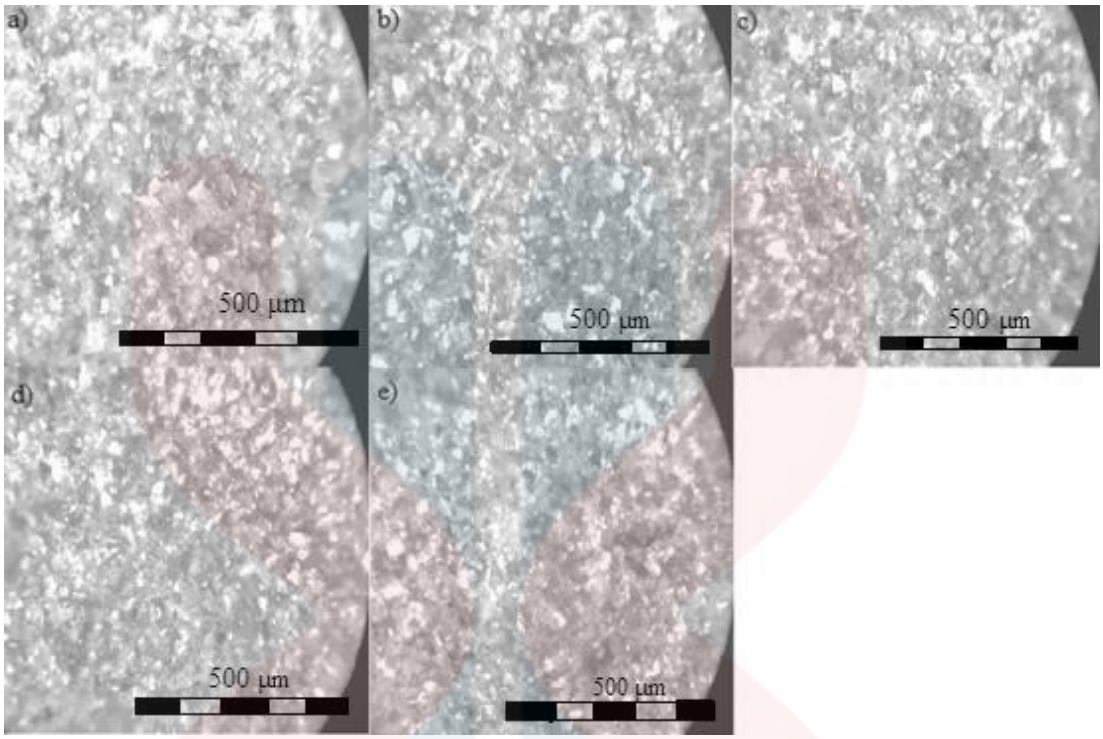

Figure 4.5: Optical microscope of composite a) SiC-10wt% feldspar b) SiC-20wt% feldspar c) SiC-30wt% feldspar d) SiC-20wt% feldspar e) SiC-10wt% feldspar

4.3.2 Phase Analysis

The XRD pattern of SiC/Feldspar composite after the sintering process. In Figure 4.6 where the sample was undergoing sintering process by using microwave. Roughly, the graph shown that the peak pattern of the XRD of all samples have equal shape with the SiC/Feldspar composite after mixing process but there were a few minor changes that happened after the sintering process.

According to the Figure 4.6, it shows that the feldspar contains lower peaks than SiC. Comparing the XRD pattern before and after mixing process, it shown that most of the highest peak was from SiC and the rest of the peak was from the feldspar and the elements for each peaks was still the same. From both of the figures, it shows that there was not having any obvious changes means that there the chemical reaction

does not occur for all of the materials. In conclusion, most of the hkl of this process was majorly the same with the previous raw materials.

By comparing Figure 4.4 and Figure 4.6, it shows a few differentiations of XRD pattern after mixing process and after sintering process. In generally, the phase peaks of SiC and feldspar was still the same but the peaks for XRD pattern after the sintering process was more sharp compared with the peaks for XRD pattern after the mixing process. This phenomenon happened because of the size of grain become more fine and small. Besides, it shows that there is no chemicals reaction before and after the mixing and sintering process.

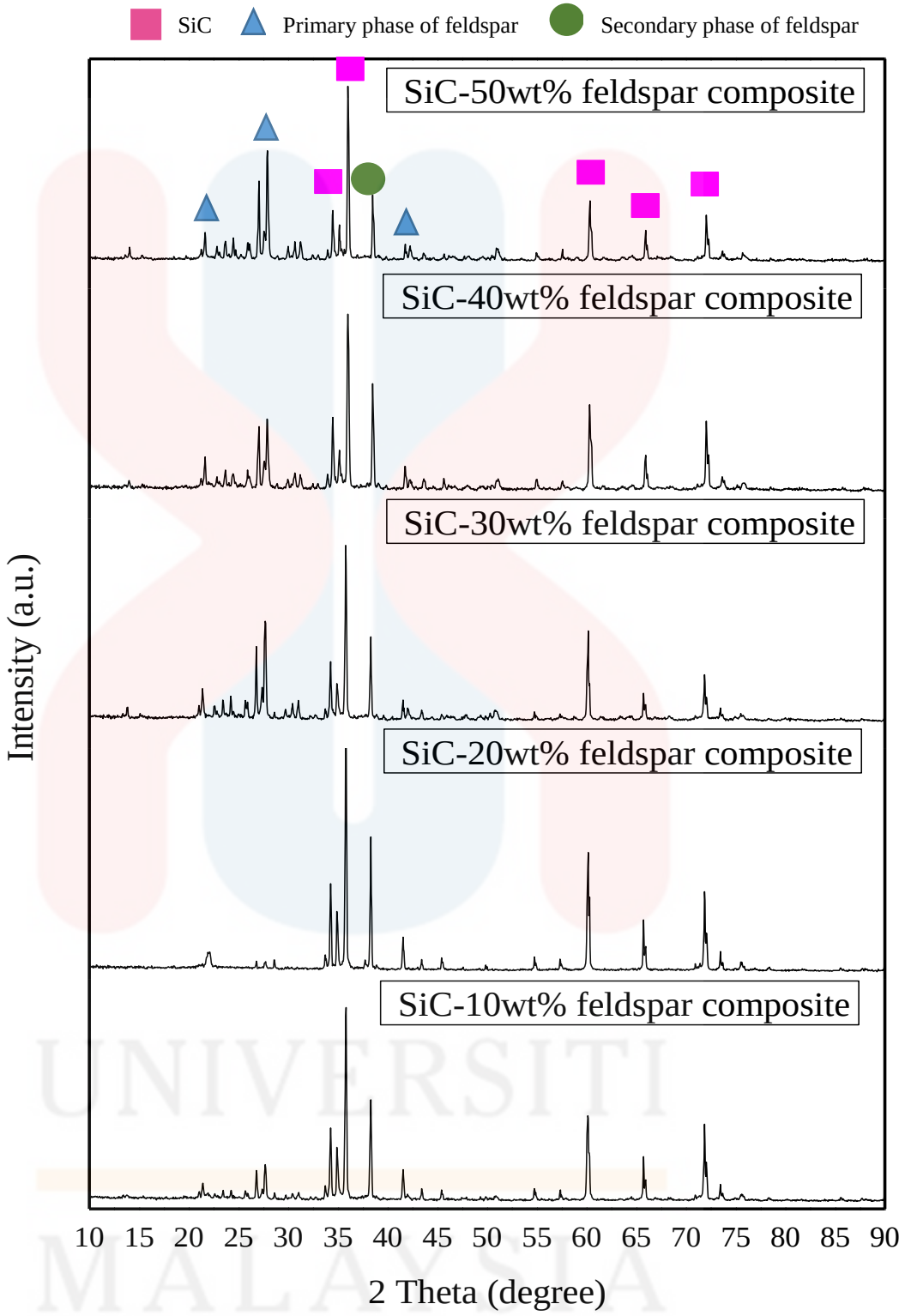

Figure 4.6: XRD pattern of SiC/Feldspar composite after sintering process at 1050˚C

4.3.3 Microwave Absorption

According to the Figure 4.7, the result shown the temperature increases during the microwave absorption. This testing was important to measure the ability of the sample to absorb heat during the sintering process. This tested was taken for 12 minutes and every 30 seconds of time was taken to observed the potential of heat absorption. This tested was using microwave oven which connected with temperature controller to help read the temperature absorb to each samples.

Figure 4.7 shown that all the sample were started with average 50˚C to 100˚C as a starting point which the graph trend steady growth until 12 minutes. The SiC-20wt% feldspar composite a having the highest recorded of microwave absorption which was 817˚C and SiC-40wt% feldspar composite was the lowest recorded of microwave absorption which was 559˚C.

This is because, the amount of matrix and reinforcement contain in the composite that become big factors the efficiencies of material to absorb the heat. In conclusion, the best composition for this testing was SiC-20wt% feldspar composite where the temperature was the highest compared to the others which was 817˚C until the final 12 minutes.

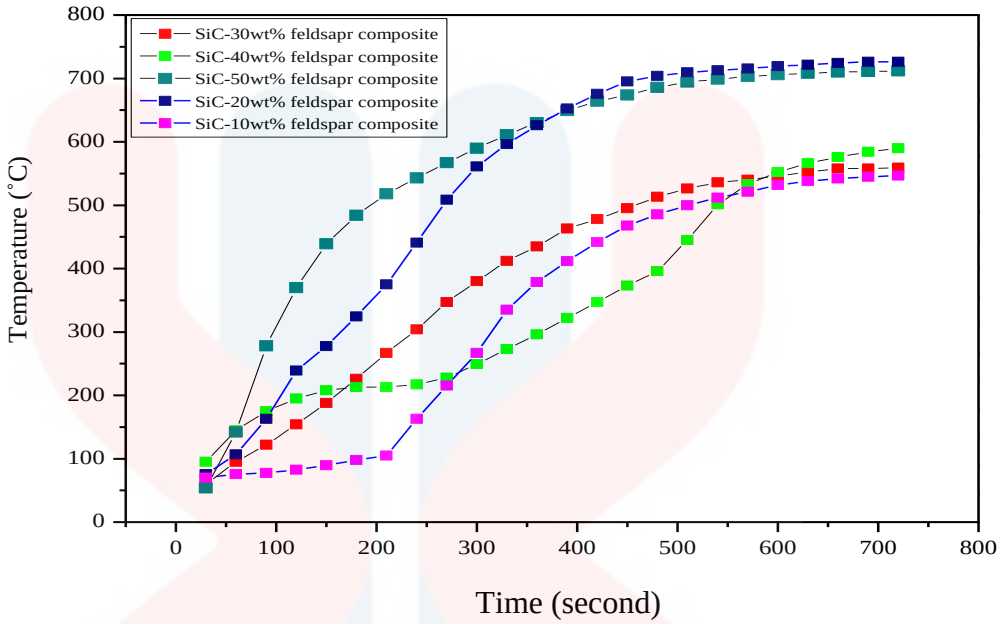

Figure 4.7: Temperature vs time for sintering process in 12 minutes

4.3.4 Density and Porous

The density and porous measurement testing was used to test the density and porous of the sample. Each of the sample needed to test with three conditions where are dry weight, suspended weight and also saturated weight to observe the weight at the different condition as discussed in Equation 3.1 and 3.2. All the test condition needed to measure for three times to get the optimum average density.

According to the Figure 4.8, it shows that the bulk density of SiC-20wt% feldspar composite which was 2.036 g/cm$^{3.}$ Then, the lightest bulk density of SiC-30wt% feldspar was 0.048 g/cm^3. The SiC-30wt% feldspar composite become very light because of the error of the equipment that effected the result during the experiment. Lastly, it can be said that the SiC-20wt% feldspar composite has the heaviest bulk density value compare with other composition.

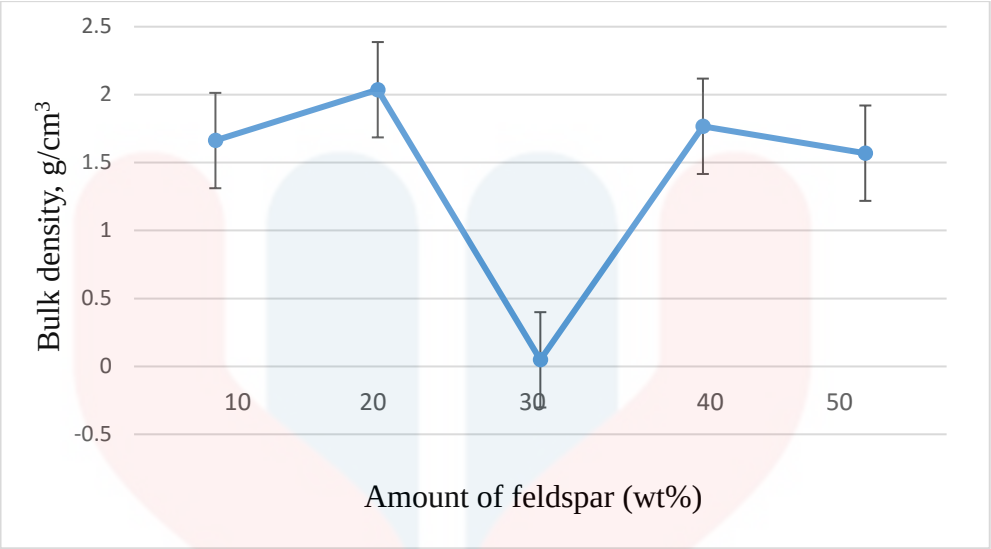

Figure 4.8: Bulk density of SiC/Feldspar composite

The sample that contain SiC-20wt% feldspar composite has the lowest apparent porosity compared with others where the percentage of porosity only 21.8%. From the graph, it shown that the density of SiC-30wt% feldspar composite was decreased drastically because of the problems that have at the equipment during the experiment running.

Based on the Figure 4.9, the result will be effected because of the previous error in Figure 4.8 result cause of the error from the equipment. Besides, there were also predicted that unseen bubbles still exist during the experiment. As a result, based on the graph 4.8 and 4.9, it can be well said that the SiC-20wt% feldspar have a high density with small size area because of the lowest porosity.

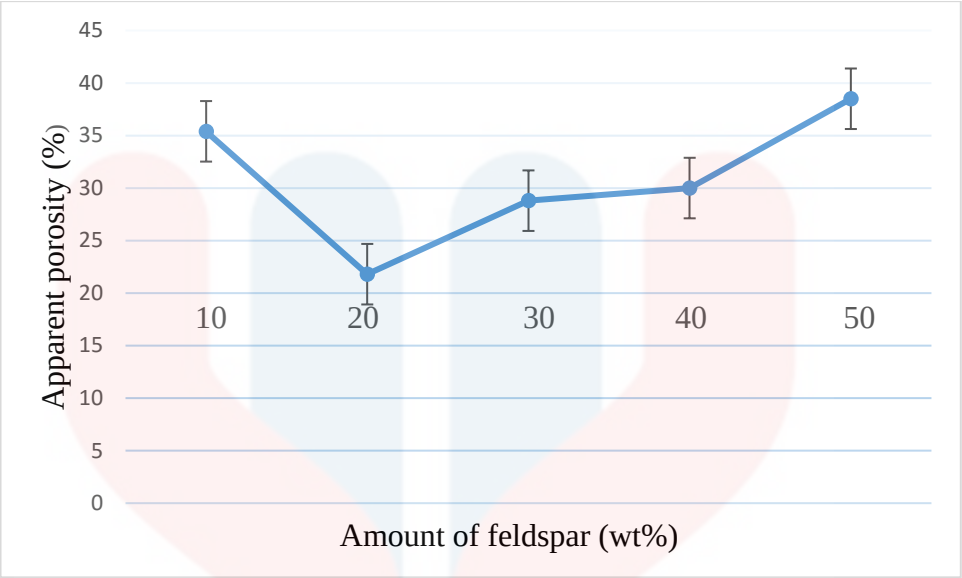

Figure 4.9: Apparent porosity of SiC/Feldspar composite

4.3.5 Dielectric Properties

4.3.5.1 Dielectric Constant

Dielectric constant of the composite is shown in Figure 4.10, SiC-20wt% feldspar composite contains the highest dielectric constant 16.6 at 1 GHz than other sample while the lowest dielectric constant was sample that contain SiC-50wt% of feldspar composite which was 13.7 at 1 GHz.

From the Figure 4.10, it shown that the SiC-50wt% of feldspar composite was very different value of dielectric constant compared to others material composition. There is unknown reason because it has many factors that need to consider such as temperature and also frequency that can affect the result. Finally, the sample which contain SiC-20wt% of feldspar composite was having highest dielectric constant compare to another sample.

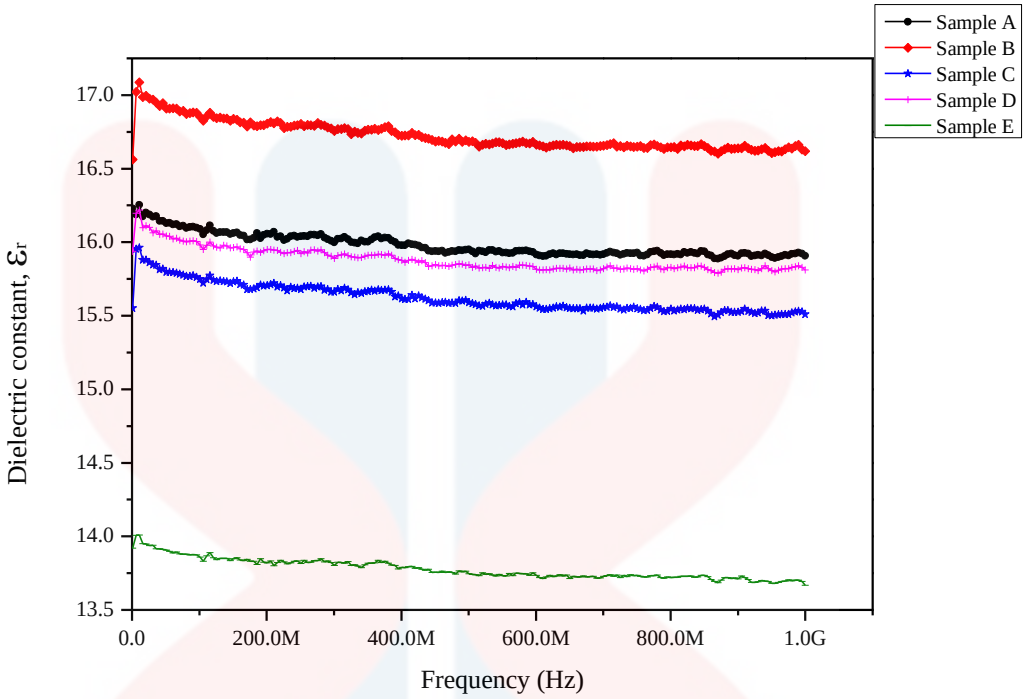

Figure 4.10: Dielectric constant of SiC/Feldspar composite

4.3.5.2 Dielectric loss

Based on the Figure 4.11, it shown that the graph of dielectric loss against with frequency. From the data recorded, it shows that the sample which having SiC-20wt% of feldspar composite is having the highest dielectric loss which is 4.07×10^{-2} compare to another sample test.

There is also unknown reason because it has many factors that need to consider such as frequency and also temperature that can affect the result. According to the graph 4.10 and 4.11, it can be concluded that when the dielectric constant high, the dielectric loss also increase.

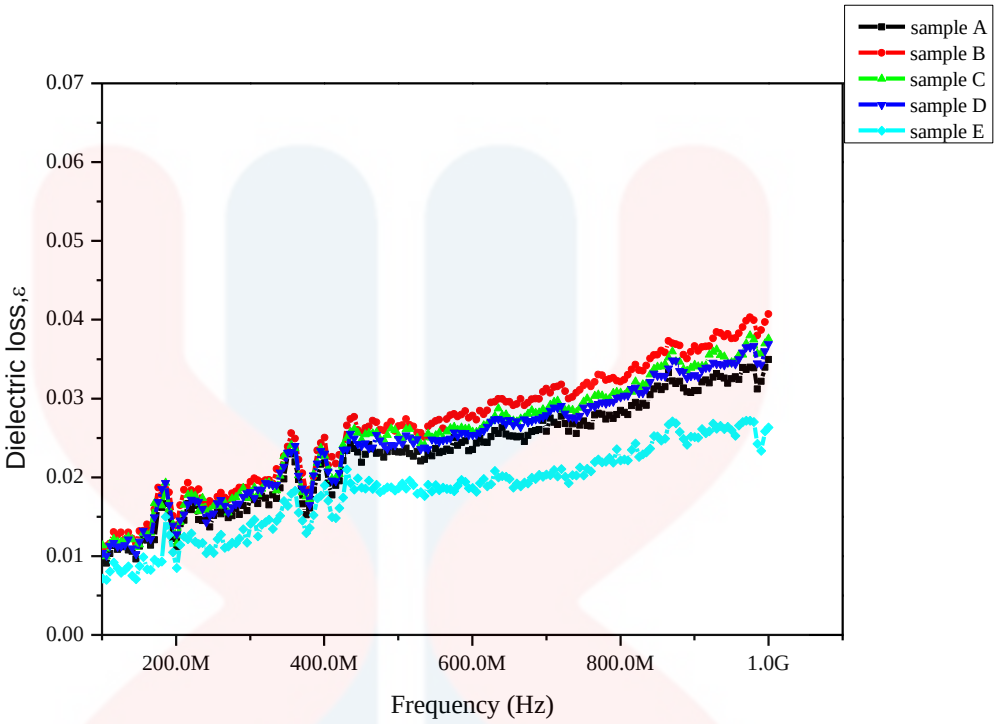

Figure 4.11: Dielectric loss of SiC/Feldspar composite

4.4 Susceptor Produced from Slip Casting and Sponge Replication

Figure 4.12, shows the comparison between the slip casting method and sponge replication method sample for microwave absorption testing. Purpose of this testing was to identify which one of the sample materials with different method that can absorb heat in 12 minutes.

As shown as Figure 4.12, it can be concluded that slip casted sample can absorbed the heat from the microwave better than sponge replication structure susceptor where the final temperature of slip casted susceptor at 12minutes was 817˚C and for the sponge replication of casted susceptor at 12 minutes was only 195˚C. This phenomenon happened because of the physical structure of slip casted susceptor that have low porous structure where the small powder particles was tried to fulfill each of the empty space while the sponge replication were having more empty space because

of the porous sponge replication structure that can be effected for microwave absorption to absorb heat. Besides, the density of the sample also effected the result of microwave absorption where slip casted sample method was denser than sponge replication method sample. As final conclusion, the slip casted surface susceptor can absorb more heat faster and efficient than porous sponge replication susceptor.

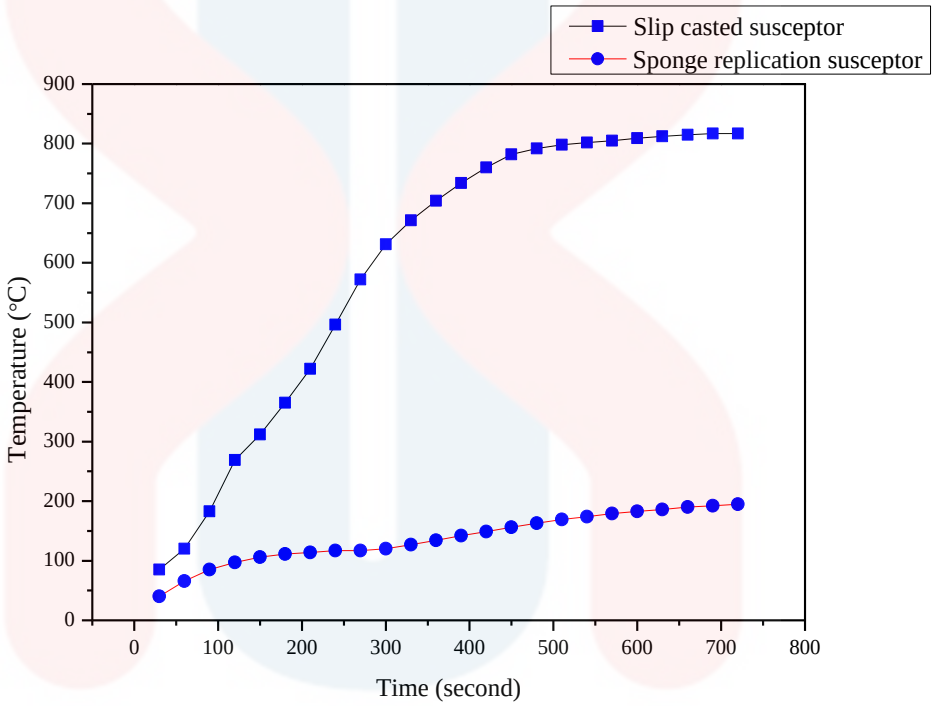

Figure 4.12: Comparison between slip casted and sponge replication susceptor for microwave absorption testing

CHAPTER 5

CONCLUSIONS AND RECOMMENDATIONS

5.1 Conclusions

In this research, the raw materials of that have been used were SiC and feldspar that will act as a matrix and reinforcement respectively to form a composite material to make susceptor for a future used.

According to the first objective, SiC/Feldspar composite was tested with five different compositions by using slip casted method and all of the composition was tested by using a few techniques to determine the properties. As a result, the best composition that recorded was SiC-20wt% feldspar composite that shown the positive result during all of the testing. Then, composition of SiC-20wt% of feldspar composite was continued with sponge replication process.

Based on second objective, all of the composition was tested by using XRD, microwave absorption, optical microscopic and dielectric test to identify more about the properties and characteristics of the composite based on different composition. According to the testing that was tested, it can be conclude that when the temperature of microwave absorption was high, the value dielectric constant and also dielectric loss also high. So that, it shows that it has a potential result to be applied in the future for many applications.

Finally, for the third objective, SiC-20wt% feldspar composite from slip casted and sponge replication method was tested by using microwave absorption to test the heat absorption on the composite material. From that comparison, it shows that the slip

casted method was more efficient than sponge replication method because it recorded 817˚C in 12 minutes.

In a conclusion based on this research, all of the objective in this thesis report was well answered. It can bravely state that the composition of composite which was 20wt% of feldspar by using slip casted method was the best sample. According to the experiment result, it having a potential to be commercialize in the industrial application because it can be used to overcome the problems.

5.2 Recommendations for A Future Research

There are a few recommendations of experiment that can be suggested for future research. First of all, to identify the clear properties of the product, impact fracture testing was suggested to use to identify the energy absorbed during fracture materials when the impact applied for the sample after firing process. From this technique, it can show which of the best composition that can give a better result for this testing. Besides, to improve the research result, the researcher can use ball milling technique to be used in the progress experiment to mix the raw materials. From this technique, it can be predicting maybe the raw materials become more homogenous and the particle size also can reduce equally. In additions, to get more information about the characteristics of the composite, the SEM technique was suggested to be used to identify more about the material 3D image appearance surface and also surface structure of the sample (Ma *et al.*, 2006).

REFERENCES

Adams, D. F. (1987). Engineering composite materials. *Composites*, *18*(3), 261.

Aigbodion, V. S., Agunsoye, J. O., Kalu, V., Asuke, F., Ola, S., Metallurgical, N., & Centre, D. (2011). Microstructure and Mechanical Properties of Ceramic Composites. *Journal of Minerals & Materials Characterization & Engineering.*, *9*(6), 527–538.

Baldacim, S. ., Cairo, C. a. ., & Silva, C. R. . (2001). Mechanical properties of ceramic composites. *Journal of Materials Processing Technology*, *119*(1–3), 273–276.

Bhattacharya, M., & Basak, T. (2016). A review on the susceptor assisted microwave processing of materials. *Energy*, *97*, 306–338.

Campbell, F. C. (2010). Introduction to Composite Materials. *Structural Composite Materials*, 1–29.

Cesnek, J., Dobias, J., Housova, J., & Sedlacek, J. (2003). Properties of Thin Metallic Films for Microwave Susceptors. *Czech Journal of Food Sciencies*, *21*(1), 34–40.

Chawla, K. K. (2012). *Composite Materials*. *Advanced Materials by Design*. New York, NY: Springer New York.

Clark, D. E., Folz, D. C., & West, J. K. (2000). Processing materials with microwave energy, *287*, 153–158.

Cornsweet, T. M. (1970). Advanced composite materials. *Science (New York, N.Y.)*, *168*(3930), 433–438.

Demirskyi, D., & Vasylkiv, O. (2016). Microstructure and mechanical properties of boron suboxide ceramics prepared by pressureless microwave sintering. *Ceramics International*, 1–5.

Deposits, Q., & Maine, O. F. (1906). Quartz and Feldspar ., 383–399.

Fagury-Neto, E., & Kiminami, R. H. G. A. (2001). Alumina/mullite/SiC powders synthesized by microwave-assisted carbothermal reduction of kaolin. *Ceramics International*, *27*(7), 815–819.

Galusek, D., Sedláček, J., Klement, R., & Švančárek, P. (2014). *Silicon carbide-containing alumina nanocomposites: processing and properties*. *Advances in Ceramic Matrix Composites*.

Gerhardt, R. (2011). *Properties and Applications of Silicon Carbide Edited by Rosario Gerhardt*.

Guo, J., Duan, Y., Liu, L., Chen, L., & Liu, S. (2011). Electromagnetic and Microwave Absorption Properties of Carbonyl-Iron/Fe91Si9 Composites in Gigahertz Range. *Journal of Electromagnetic Analysis and Applications*, *3*(5), 140–146.

Hu, N. (2006). Composites, *12*(2), 0–5.

Jones, R. H. (2001). Metal Matrix Composites. *Environmental Effects on Engineered Materials*, *40*(1), 375–390.

Low, I. M. (2014). *1 - Advances in ceramic matrix composites: an introduction*. *Advances in Ceramic Matrix Composites*. Woodhead Publishing Limited.

M. S. Sharmiwati, R. M. Mizan, a. B. N. (2014). Preparation And Characterization Of Ceramic Sponge For Water Filter. *International Journal of Scientific & Technology Research*, *3*(6), 103–106.

Ma, H., Shieh, K., & Qiao, T. X. (2006). Study of Transmission Electron Microscopy (TEM) and Scanning Electron Microscopy (SEM). *Nature and Science*, *4*(3), 14–22.

Mandal, P. R., & Nath, T. K. (2014). Enhanced magnetocapacitance and dielectric

property of Co ZnFeO-PbZr TiO magnetodielectric composites. *Journal of Alloys and Compounds*, *599*, 71–77.

Marx, K. (1992). 1. Etymology. *Natural History*, 1–7.

Mazumdar, S. K. (1998). *Handbook of Composites*. (S. T. Peters, Ed.)*CRC press LCC* (Vol. 32). Boston, MA: Springer US. Mecânica, S. D. T., Técnico, I. S., & Pais, A. R. (2015). Conversion of a commercial microwave oven to a sintering furnace controlled by computer Gonçalo Leonel, 1–10.

Moissan, H. (1907). Silicon carbide Discovery and early production Early experiments, 1–11.

Naga, S. M. (2014). Ceramic matrix composite thermal barrier coatings for turbine parts. In *Advances in Ceramic Matrix Composites* (pp. 524–536). Elsevier.

National, I., & Recherche, D. (2008). Silicon Carbide : Synthesis and Properties, (C), 361–389.

Perry, M. R., & Lentz, R. R. (2009). Susceptors in microwave packaging. *Development of Packaging and Products for Use in Microwave Ovens*, 207–236.

Plains, S., & Plains, S. (2012). Table of Contents. *The Journal of Prosthetic Dentistry*, *107*(5), A4–A6.

Reddy, M. P., Ubaid, F., Shakoor, R. A., Mohamed, A. M. A., & Madhuri, W. (2016). Journal of Science : Advanced Materials and Devices Structural and mechanical properties of microwave sintered Al Ni 50 Ti 50 composites. *Journal of Science: Advanced Materials and Devices*, *1*(3), 362–366.

Sulaiman, M. a, Hutagalung, S. D., Ahmad, Z. a, Mohamed, M., Yusof, M., & Mamat, S. (2014). Enhanced Electromagnetic Absorption on Formulated SiC-Al 2 O 3 Composite Crucible. *International Journal of Electroactive Materials*, *2*, 1–3.

Tejaswi, V. (2012). Mechanical properties of polymer composite materials, 78–81.

Tiwari, N. (2015a). introduction to Composite Materials and Structures. *Institute of Technology Kanpur*, *2012*.

Tiwari, N. (2015b). Introduction to Composite Materials and Structures Lecture 1 Introduction.

Vargas, E., Pantoya, M. L., Saed, M. A., & Weeks, B. L. (2016). Advanced susceptors for microwave heating of energetic materials. *Materials & Design*, *90*, 47–53.

Venkatesh, B., & Harish, B. (2015). MECHANICAL PROPERTIES OF METAL MATRIX COMPOSITES (Al/SiCp) PARTICLES PRODUCED BY POWDER METALLURGY. *International Journal of Engineering Research and General Science*, *3*(1), 1277–1284.

Vinet, L., & Zhedanov, A. (2010). A "missing" family of classical orthogonal polynomials. *Materials & Design*, *17*(1), 56. Wang, R.-M., Zheng, S.-R., & Zheng, Y.-P. (2011). Introduction to polymer matrix composites. *Polymer Matrix Composites and Technology*, 1–548.

Wong, W., & Gupta, M. (2015). Using Microwave Energy to Synthesize Light Weight/Energy Saving Magnesium Based Materials: A Review. *Technologies*, *3*(1), 1–18.

Yin, L., & Stoll, R. (2014). *Ceramics in restorative dentistry*. *Advances in ceramic matrix composites* (Vol. 1). Woodhead Publishing Limited.

Zhao, J. (2014). *The use of ceramic matrix composites for metal cutting applications*. *Advances in Ceramic Matrix Composites*. Woodhead Publishing Limited.

APPENDICES A

RAW MATERIALS

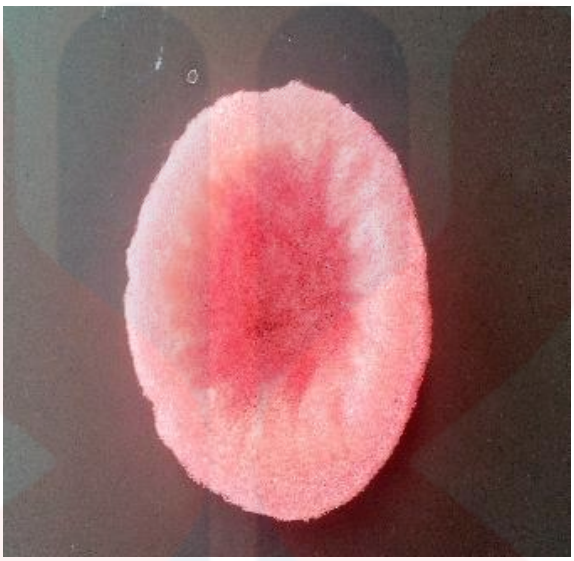

Figure A. 1: Porous sponge

Pattern: COD 9010158 (Tune Cell) Radiation: 1.54060 Quality: User modified

Formula	C Si
Name	
Name (mineral)	Moissanite
Name (common)	
Lattice:	Hexagonal
S.G.:	P 63 m c (186)
Mol. weight =	
Volume [CD] =	124.34
Dx =	
Dm =	
I/Icor =	1.480
a = 3.08100	alpha =
b =	beta =
c = 15.12480	gamma =
a/b = 1.00000	Z =
c/b = 4.90906	

Primary Reference
Capitani G. C., Di Pierro S., Tempesta G., "The 6H-SiC structure model: Further refinement from SCXRD data from a terrestrial moissanite Locality: 150 km NW from Izmir, Turkey", American Mineralogist 92 (2007) 403-407.

Radiation:	
Wavelength:	1.54060
SS/FOM:	
Filter:	Not specified
d-spacing:	

d	2θ	I	h	k	l
2.62765	34.093	1527	-1	0	-1
2.52080	35.586	1838	0	0	-6
2.51620	35.653	2725	-1	0	-2
2.35831	38.129	1623	-1	0	-3
2.18009	41.383	649	-1	0	-4
2.00102	45.282	251	-1	0	-5
1.67917	54.612	325	-1	0	-7
1.54261	59.914	802	-1	0	-8
1.54050	60.004	1590	-2	1	0
1.42199	65.600	709	-1	0	-9
1.32895	70.849	139	-2	0	-1
1.31579	71.667	289	-1	0	-10
1.31448	71.749	1176	-2	1	-6
1.31382	71.790	292	-2	0	-2
1.28972	73.348	235	-2	0	-3
1.26040	75.346	85	0	0	-12
1.25810	75.508	123	-2	0	-4
1.22224	78.135	49	-1	0	-11
1.22067	78.255	49	-2	0	-5
1.13516	85.466	79	-2	0	-7
1.09004	89.929	240	-2	0	-8
1.06647	92.487	33	-1	0	-13
1.04489	94.988	262	-2	0	-9
1.00626	99.904	120	-3	1	-1

Figure A. 8: COD 9010158 pattern by using XRD technique

Pattern: COD 9004191 (Tune Cell) Radiation: 1.54060 Quality: User modified

Formula	Al K0.95 Na0.05 O8 Si3
Name	
Name (mineral)	Microcline
Name (common)	

Lattice:	Triclinic			Mol. weight =	
S.G.:	C -1 (2)			Volume [CD] =	721.3
				Dx =	
				Dm =	
				I/Icor =	0.630
a =	8.57140	alpha =	90.600		
b =	12.96460	beta =	115.90		
c =	7.22170		0		
a/b =	0.66114	gamma =	87.700		
c/b =	0.55703	Z =			

Primary Reference
Blasi A., De Pol Blasi C., Zanazzi P. F., "A re-examination of the Pellotsalo microcline: Mineralogical implications and genetic considerations", The Canadian Mineralogist 25 (1987) 527-537.

Radiation:		Filter:	Not specified
Wavelength:	1.54060	d-spacing:	
SS/FOM:			

d	2θ	I	h	k	l	d	2θ	I	h	k	l
6.7398 4	13.125	54	-1	-1	0	2.8943 4	30.869	42	0	-2	2
6.5096 5	13.592	9	-1	1	0	2.8892 2	30.925	99	0	-4	1
6.4961 4	13.620	39	0	0	-1	2.8172 9	31.736	2	-2	0	-1
6.4768 8	13.661	44	0	-2	0	2.7830 8	32.136	78	-1	-3	2
5.9292 8	14.929	63	-1	-1	1	2.7817 6	32.391	10	-3	1	1
5.8069 4	15.246	31	-1	1	1	2.7563 8	32.456	115	-1	3	2
4.6047 5	19.260	31	0	-2	-1	2.6203 0	34.192	77	-3	-1	2
4.2190 8	21.040	596	-2	0	1	2.6176 7	34.227	153	-2	-4	1
3.9848 1	22.292	145	-1	-1	-1	2.6145 6	34.269	8	-2	-2	-1
3.9242 8	22.640	62	-1	1	-1	2.5849 9	34.674	102	-3	1	2
3.8522 2	23.070	54	-2	0	0	2.5705 8	34.874	70	-1	-1	-2
3.8318 5	23.194	340	-1	-3	0	2.5534 6	35.116	23	-2	2	-1
3.7047 5	24.001	341	-1	3	0	2.5510 1	35.151	28	-1	1	-2
3.6537 0	24.342	113	-1	-3	1	2.5383 3	35.332	41	-3	-1	0
3.5986 1	24.720	102	-2	-2	1	2.5286 0	35.472	13	-2	-4	0
3.5881 9	24.934	50	-1	3	1	2.5228 1	35.557	192	-2	4	1
3.4864 5	25.529	286	-1	-1	2	2.5003 3	35.887	45	-3	1	0
3.4750 1	25.614	14	-2	2	1	2.4321 6	36.929	58	-1	-5	1
3.4688 3	25.660	221	-1	1	2	2.4319 7	36.932	19	-2	4	0
3.3699 2	26.427	486	-2	-2	0	2.4268 2	37.013	1	-1	5	0
3.2904 4	27.077	536	-2	0	2	2.4251 8	37.039	73	-3	-3	1
3.2548 3	27.379	448	-2	2	0	2.3897 4	37.609	28	-1	5	1
3.2480 7	27.438	725	0	0	-2	2.3384 6	38.465	2	-2	-4	2
3.2384 4	27.521	298	0	-4	0	2.3365 8	38.498	38	-3	3	1
3.0331 5	29.424	244	-1	-3	-1	2.3345 3	38.533	28	-1	-1	3
2.9648 4	30.120	46	-2	-2	2	2.3315 8	38.583	33	-1	1	3
2.9543 9	30.227	305	-1	3	-1	2.3023 8	39.092	2	0	-4	-2
2.9126 1	30.671	57	0	-2	-2	2.2983 0	39.165	16	-3	-3	2
2.9073 9	30.727	139	0	-4	-1	2.2548 7	39.951	1	-1	-3	-2
2.9034 7	30.770	23	-2	2	2	2.2488 8	40.062	7	-2	-2	3

Figure A.9: COD 9004191 pattern by using XRD technique

Pattern: COD 9013308 (Tune Cell) Radiation: 1.54060 Quality: User modified

Formula	Al1.1 Ca0.1 K0.27 Na0.63 O8 Si2.9
Name	
Name (mineral)	Anorthoclase
Name (common)	

Lattice:	Triclinic	Mol. weight =	
S.G.:	C -1 (2)	Volume [CD] =	686.97
		Dx =	
		Dm =	
		I/Icor =	0.730

a =	8.27800	alpha =	91.790
b =	12.94900	beta =	116.160
c =	7.14500	gamma =	90.190
a/b =	0.63928	Z =	
c/b =	0.55178		

Pressure of data collection: 100.00 kPa:

Primary Reference
Nestola F., Curetti N., Benna P., Ivaldi G., Angel R., Bruno E., "Compressibility and high-pressure behavior of Ab63Or27An10 anorthoclase Locality: Torino, Italy Note: P = 0.0001 GPa", The Canadian Mineralogist 46 (2008) 1443-1454.

Radiation:		Filter:	Not specified
Wavelength:	1.54060	d-spacing:	
SS/FOM:			

d	2θ	I	h	k	l	d	2θ	I	h	k	l
6.49622	13.620	8	-1	1	0	2.84658	31.401	4	0	-4	-1
6.47017	13.675	48	0	-2	0	2.83083	31.580	16	0	-2	-2
6.40885	13.806	28	0	0	-1	2.79396	32.008	27	-1	-3	2
6.39023	13.847	1	-1	-1	0	2.70896	33.040	30	-1	3	2
5.82987	15.185	42	-1	-1	1	2.69688	33.193	4	-3	1	1
5.73659	15.434	52	-1	1	1	2.69082	33.270	3	-3	-1	1
4.63854	19.118	4	0	-2	1	2.54458	35.242	11	-2	2	-1
4.09064	21.708	232	-2	0	1	2.54270	35.269	25	-3	-1	2
3.90142	22.775	228	-1	1	-1	2.54028	35.304	51	-2	-4	1
3.82785	23.218	253	-1	-1	-1	2.53466	35.385	36	-2	4	1
3.78146	23.634	207	-1	3	0	2.53341	35.403	20	-3	1	2
3.71435	23.938	15	-2	0	0	2.52866	35.472	47	-1	1	-2
3.69974	24.034	162	-1	-3	0	2.49454	35.973	35	-1	-1	-2
3.62183	24.559	52	-1	-3	1	2.49124	36.022	12	-2	-2	-1
3.55499	25.028	25	-1	3	1	2.46286	36.452	3	-2	4	0
3.47001	25.652	170	-1	-1	2	2.44070	36.795	41	-3	1	0
3.46113	25.719	13	-2	-2	1	2.42360	37.064	40	-3	-1	0
3.45402	25.772	12	-2	2	1	2.41954	37.128	28	-1	-5	1
3.41451	26.076	198	-1	1	2	2.41682	37.172	9	-2	-4	0
3.24811	27.437	252	-2	2	0	2.38609	37.668	36	-1	5	1
3.23508	27.550	157	0	-4	0	2.35442	38.194	7	-2	0	3
3.23199	27.577	257	-2	0	2	2.32718	38.659	20	-3	3	1
3.20443	27.819	632	0	0	-2	2.31927	38.796	4	0	-4	2
3.19512	27.901	230	-2	-2	0	2.31554	38.861	21	-3	-3	1
3.00253	29.731	208	-1	3	-1	2.30987	38.961	7	-2	-4	2
2.93128	30.471	31	0	-4	1	2.29507	39.222	1	-1	1	3
2.91493	30.646	34	-2	-2	2	2.29684	40.287	11	-1	3	-2
2.91408	30.655	49	0	-2	2	2.23627	40.297	7	0	-4	-2
2.90408	30.763	212	-1	-3	-1	2.23273	40.364	4	-2	-2	3
2.88830	31.157	24	-2	2	2	2.21445	40.712	34	-1	5	-1

Figure A. 4: COD 9013308 pattern by using XRD technique

APPENDICES B

RAW DATA

Table B. 1: Temperature taken of microwave absorption testing

Time (sec)	Temperature (˚C)				
	10wt% of feldspar	**20wt% of feldspar**	**30wt% of feldspar**	**40wt% of feldspar**	**50wt% of feldspar**
30	60	85	95	79	54
60	95	120	145	85	142
90	122	183	175	87	278
120	154	269	195	93	370
150	188	312	208	101	439
180	226	365	213	110	484
210	267	422	213	118	518
240	304	496	217	183	543
270	347	572	228	242	567
300	380	631	249	300	590
330	412	671	273	377	611
360	435	704	296	426	630
390	463	734	322	463	649
420	478	760	347	497	664
450	495	782	373	526	674
480	513	792	396	546	686
510	526	798	445	562	694
540	536	802	501	576	699
570	540	805	533	586	703
600	546	809	552	598	706
630	552	812	566	605	708
660	558	815	576	610	710
690	558	817	584	613	711
720	559	817	590	615	712

Table B.2: Reading of density and porous measurement

Amount of feldspar (wt%)	Reading of dry weight (g/cm^3)	Reading of suspended weight (g/cm^3)	Reading of saturated weight (g/cm^3)
10	0.108	0.066	0.131
	0.109	0.065	0.132
	0.108	0.066	0.131
Average	**0.108**	**0.066**	**0.131**
20	0.112	0.071	0.125
	0.114	0.069	0.123
	0.112	0.068	0.125
Average	**0.112**	**0.069**	**0.124**
30	0.108	0.064	0.122
	0.107	0.066	0.125
	0.107	0.065	0.125
Average	**0.107**	**0.065**	**0.124**
40	0.107	0.065	0.123
	0.104	0.062	0.122
	0.106	0.064	0.126
Average	**0.106**	**0.064**	**0.124**
50	0.105	0.064	0.128
	0.101	0.060	0.127
	0.100	0.062	0.127
Average	**0.102**	**0.062**	**0.127**

Table B.2: Sponge replication susceptor of microwave absorption testing

Time (second)	Temperature (˚C)
30	40
60	66
90	85
120	97
150	106
180	111
210	114
240	117
270	117
300	120
330	127
360	134
390	142
420	149
450	156
480	163
510	169
540	174
570	179
600	183
630	186
660	190

690	192
720	195

APPENDIXES C

SAMPLE PRODUCTS AND TESTING

Figure C. 1: Slip casting process

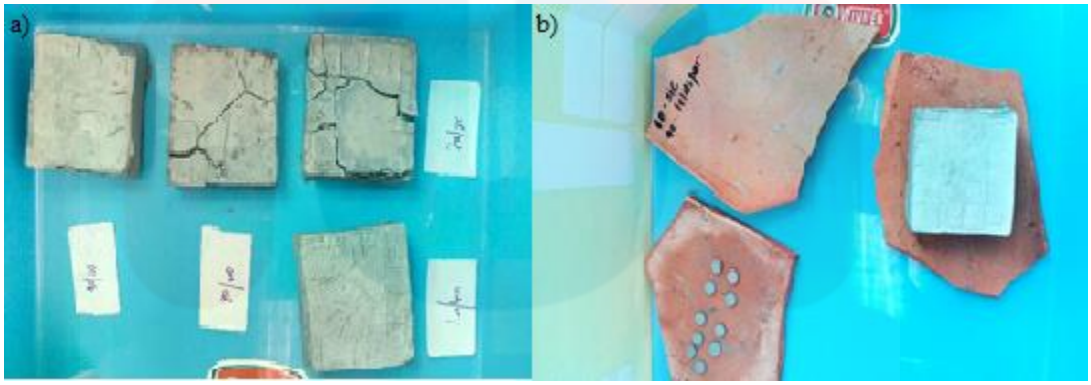

Figure C. 2: Sample after firing process a) SiC/Feldspar composite b) SiC/Feldspar composite and pellet

Figure C. 3: Sample in microwave absorption testing